ACR Jan. 1943

NATIONAL ADVISORY COMMITTEE FOR AERONAUTICS

# WARTIME REPORT

ORIGINALLY ISSUED
January 1943 as
Advance Confidential Report

## WIND-TUNNEL INVESTIGATION OF A PLAIN AILERON WITH THICKENED AND BEVELED TRAILING EDGES ON A TAPERED LOW-DRAG WING

By Paul E. Purser and John W. McKee

Langley Memorial Aeronautical Laboratory
Langley Field, Va.

NACA

WASHINGTON

NATIONAL ADVISORY COMMITTEE FOR AERONAUTICS

ADVANCE CONFIDENTIAL REPORT

# WIND-TUNNEL INVESTIGATION OF A PLAIN AILERON WITH THICKENED AND BEVELED TRAILING EDGES ON A TAPERED LOW-DRAG WING

By Paul E. Purser and John W. McKee

## SUMMARY

An investigation was made in the LMAL 7- by 10-foot tunnel of various modifications of the trailing-edge portion of a 0.20-chord plain aileron on a partial-span model of a tapered low-drag wing. The modifications considered consisted of various amounts of symmetrical and unsymmetrical thickening and beveling of the aileron trailing edge. The effects of aileron-nose gap, nose-seal location, and tab deflection were determined for the most promising modifications. The control-wheel forces and the rates of roll were estimated for a high-speed airplane with the original aileron and with some of the modified ailerons.

The results of the tests indicated that, for the arrangement tested, the use of beveled ailerons would substantially reduce the high-speed control forces and would cause some changes in the airplane stability characteristics. Although not directly comparable, the results are in qualitative agreement with previous wind-tunnel and flight tests. The effects of profile modifications on the hinge-moment characteristics appeared to depend greatly on the included angle between the upper and lower surface at the aileron trailing edge. Air leakage across the aileron nose tended to cause overbalance of the beveled ailerons at small deflections and also to reduce their rolling-moment effectiveness. This leakage caused a greater loss of effectiveness with the beveled aileron profile than with the original cusp aileron profile. Thickening and beveling only one surface of the aileron gave less aerodynamic balance than thickening and beveling both surfaces and produced a larger floating tendency, which would allow advantageous use of a differential aileron linkage. Tab effectiveness varied with aileron

profile and in some cases was unsatisfactory. An alternative trimming device that should prove satisfactory when the use of an ordinary tab is inadvisable is suggested and analyzed.

## INTRODUCTION

The increased importance of obtaining adequate lateral control with reasonable control forces for high-speed airplanes under all flight conditions has led the NACA to engage in an extensive program of lateral-control research. The purposes of this program are to determine the characteristics of existing lateral-control devices, to determine the effects of various modifications to existing devices, and to develop new devices that show promise of being more satisfactory than those now in use.

Two-dimensional-flow tests of a 30-percent-chord plain flap on an NACA 0009 airfoil (reference 1), three-dimensional-flow tests of a 15.5-percent-chord plain aileron on a tapered NACA 230 series wing (reference 2), and unpublished results of flight tests of a fighter airplane show that thickening and beveling the control-surface trailing edge is a powerful means of adjusting the hinge-moment characteristics. The present tests were made to determine the effects of various profile modifications on the characteristics of an aileron on a tapered-wing model with low-drag airfoil sections.

## APPARATUS AND METHODS

### Model

The basic wing model (figs. 1 and 2) was a 0.40-scale partial-span model of a low-drag wing, built of laminated mahogany. The airfoil section varied from NACA 66,2-2(13.716) at the root to NACA 66,2-2(13.125) near the tip.

The 0.20c aileron and typical aileron profile modifications tested are shown in figure 3. The true aileron profile for this low-drag wing is a cusp. All variations from the cusp or true profile ended abruptly at the inboard end of the aileron and faired into the tip. The aileron was tested with a sheet rubber seal in two locations. This seal prevented air flow across the nose of the aileron from the

inboard hinge to the outboard hinge but did not seal the 0.02-inch longitudinal gaps at the hinges. In order to form the beveled aileron contours the original aileron was first thickened to straight lines tangent to the nose arcs and passing through points 1 percent of the wing chord above and below the original upper and lower surfaces at the aileron trailing edge. The trailing-edge portion was then beveled linearly and symmetrically to the original trailing-edge thickness. The beveled portion of the aileron will hereinafter be referred to as the "bevel." The junctures between the forward and rearward parts of the aileron were rounded by arcs with radii equal to 20 percent of the wing chord. (See fig. 3.)

The geometric characteristics of the low-drag wing and of the 0.40-scale model are given in table I.

## Test Installation

The test setup is shown schematically in figure 4. The partial-span wing model was supported horizontally in the LMAL 7- by 10-foot tunnel (reference 3) with the inboard end of the model adjacent to one of the vertical walls of the tunnel, the tunnel wall thereby serving as a reflection plane. The model was supported entirely on the balance frame with a small clearance at the tunnel wall so that all the forces and moments acting upon the model might be measured. The angle of attack of the model could be changed while the tunnel was in operation.

The aileron was deflected and the hinge moments were measured by means of a calibrated torque rod and linkage system developed for this type of test setup (fig. 5). Torque to deflect the aileron is applied at the hinge-moment dial and transmitted by the torque rod, the aileron-deflection-drive tube, and the link to the aileron. The aileron deflection is indicated on the aileron-deflection dial by a pointer fixed with respect to the wing. The aileron hinge moment is determined from the twist in the torque rod, which is indicated on the hinge-moment dial. Inasmuch as a clamp is provided for locking the hinge-moment dial to the balance frame for each aileron deflection, no external loads are imposed upon the balance system. The torque rod is calibrated in the actual installation for each model tested.

## Test Condition

All tests were made at a dynamic pressure of 16.37 pounds per square foot, which corresponds to a velocity of about 80 miles per hour, and at a test Reynolds number of about 2,350,000, based on the mean aerodynamic chord of a complete 0.40-scale model (3.21 ft). The tests were made at low scale, low velocity, and high turbulence relative to the flight conditions to which the results are applied. The effects of these variables were not determined or estimated.

# RESULTS AND DISCUSSION

## Coefficients and Corrections

The symbols used in the presentation of the results are:

$C_L$ lift coefficient ($L/qS'$)

$C_D$ drag coefficient ($D/qS'$)

$C_{l'}$ rolling-moment coefficient ($L'/qbS$)

$C_{l'_m}$ uncorrected model rolling-moment coefficient $\left(\frac{L'_m}{qb'S'}\right)$

$C_{n'}$ yawing-moment coefficient ($N'/qbS$)

$C_h$ aileron hinge-moment coefficient ($H/qS_a\bar{c}_a$)

L twice lift of partial-span model

D twice drag of partial-span model

L' rolling moment about wind axis in plane of symmetry of complete wing due to aileron deflection

$L'_m$ uncorrected rolling moment of partial-span model about wind axis at tunnel wall due to aileron deflection

N' yawing moment about wind axis in plane of symmetry of complete wing due to aileron deflection

H aileron hinge moment

c wing chord

$c_a$ aileron chord aft of hinge axis (measured perpendicular to hinge axis)

$\bar{c}_a$ root-mean-square chord of aileron (measured perpendicular to hinge axis)

$b$ span of complete wing

$b'$ twice span of partial-span model

$S$ area of complete wing

$S'$ twice area of partial-span model

$S_a$ area of one aileron aft of hinge axis

$\alpha$ angle of attack of wing

$\delta_a$ aileron deflection from neutral, positive when trailing edge is down

$\delta_t$ tab deflection relative to aileron, positive when trailing edge is down

$\theta_w$ control-wheel deflection

$q$ dynamic pressure of airstream, uncorrected for blocking $\left(\frac{1}{2}\rho V^2\right)$

$V$ free-stream velocity

$V_i$ indicated velocity

$C_{l'_p}$ rate of change of rolling-moment coefficient $C_{l'}$ with helix angle $pb/2V$

$p$ rate of roll

$F_w$ aileron control-wheel force

Subscripts:

$u$ aileron-up condition

$d$ aileron-down condition

A positive value of $L'$ or $C_{l'}$ corresponds to an increase in lift of the model, and a positive value of $N'$

or $C_n'$ corresponds to a decrease in drag of the model. The angle of attack, drag coefficient, and rolling-moment coefficient have been corrected for the effect of the tunnel boundaries and to the aspect ratio and taper ratio of the complete wing. The over-all corrections to the hinge- and yawing-moment coefficients were estimated to be small and were not applied. No corrections have been applied to any of the results for blocking, for the effects of the support strut, or for the treatment of the inboard end of the model, that is, for the small gap between the model and the wall, for the leakage through the wall around the support tube, or for the boundary layer at the wall.

The over-all corrections which were applied (by addition) to the angle of attack (in deg), the drag coefficient, and the rolling-moment coefficient were:

$$\Delta\alpha^\circ = 0.41\ C_L$$

$$\Delta C_D = 0.0084\ C_L^2$$

$$\Delta C_l' = -0.319\ C_{l'_m}$$

## Characteristics with Ailerons Neutral

Effect of aileron profile.- The characteristics of the 0.40-scale model with the various ailerons set at zero are shown in figures 6 to 8. The changes in lift and drag coefficients of the complete wing caused by modifications of the aileron profile should be less than indicated by the figures since the percentage of span covered by the aileron would be less on the complete wing than on the partial-span model. Thickening the aileron profile reduced the slope of the lift curve. Thickness added to the aileron lower surface had a much greater effect on the lift-curve slope than did a similar modification of the aileron upper surface. Modifications of the aileron profile had no measurable effect on the minimum drag coefficient under the test conditions of low scale and high turbulence. The slope of the hinge-moment curve $\partial C_h/\partial\alpha$ at zero angle of attack became more positive as the aileron profile was thickened and, for symmetrical thickening, appeared to vary directly with changes in the included angle between upper and lower surfaces of the aileron at the trailing edge. The data of references 1 and 2 showed similar variations of $\partial C_h/\partial\alpha$ with trailing-edge angle.

Effect of nose gap and seal.- The effects of gaps and seals at the aileron nose may be determined by comparisons of the data from figures 6 to 8 and are summarized for the original cusp aileron and for one beveled aileron in figures 9 and 10. The presence of a seal at the aileron nose had no appreciable effect on the wing or aileron characteristics except in the case of the original cusp aileron, for which the seal slightly increased the slope of the lift curve.

## Characteristics with Ailerons Deflected

Effect of aileron profile.- The effects on the aileron characteristics of modifications of the aileron profile are shown in figures 11 to 15. As the aileron profile was thickened the slope of the hinge-moment curve $\partial C_h/\partial \delta_a$ became more positive and the rolling-moment coefficient available from a given aileron deflection decreased. Changes in the aileron profile had no appreciable effect on the yawing-moment coefficients. Thickening the aileron on only the upper or lower surface had approximately half the effect on $\partial C_h/\partial \delta_a$ as thickening both surfaces and produced changes of about $16^\circ$ in aileron floating angle at a low angle of attack. At high angles of attack, the aileron with the bevel on only the lower surface had almost the same characteristics as the symmetrically beveled aileron; whereas the aileron with the bevel on only the upper surface had characteristics that approached those of the original cusp aileron. At a low angle of attack, additional thickness on the top of the aileron had very little effect at high positive aileron deflections and additional thickness on the bottom of the aileron had very little effect at high negative deflections. For the sealed ailerons with symmetrically thickened profiles, $\partial C_h/\partial \delta_a$ appeared to vary directly with changes in trailing-edge angle. The data of references 1 and 2 showed similar variations of $\partial C_h/\partial \delta_a$ with trailing-edge angle.

Effect of nose gap and seal.- The effects of gaps and seals at the aileron nose may be determined by comparisons of the data from figures 11 to 13 and are summarized for the original cusp aileron and two of the beveled ailerons in figures 16 to 18. At a low angle of attack, the presence of the seal provided a 12-percent increase in the increment of rolling-moment coefficient between $\delta_a = 15^\circ$ and $\delta_a = -15^\circ$ for the original cusp aileron. The bottom seal slightly increased the negative value of $\partial C_h/\partial \delta_a$

while the top seal reduced this value by about 0.002 at a low angle of attack. At a low angle of attack the aileron with the $0.20c_a$ bevel was considerably overbalanced with no seal; the addition of the top seal reduced this overbalance to about half the no-seal value, and moving the seal to the bottom location produced a slightly negative value of $\partial C_h/\partial \delta_a$. The presence of the seal caused a 20-percent increase in the increment of rolling-moment coefficient between $\delta_a = 15^\circ$ and $\delta_a = -15^\circ$. The aileron with the $0.30c_a$ bevel was overbalanced with no seal and large gaps but, when the gaps were reduced by one-half either with or without plasticine to change their internal shape, $\partial C_h/\partial \delta_a$ became nearly zero. Adding the bottom seal to the aileron changed $\partial C_h/\partial \delta_a$ to a negative value of the same order of magnitude as the positive value obtained for the aileron with the large gap. Reducing the gaps by half increased the increment of rolling-moment coefficient between $\delta_a = 15^\circ$ and $\delta_a = -15^\circ$ by about 16 percent; sealing the nose increased the increment by about 28 percent.

Effect of seal location.- The effects of changing the seal location on the aileron characteristics may be determined from figures 16 to 19. The location of the seal had no measurable effects on the aileron rolling- and yawing-moment coefficients. As shown in figure 19, the aileron profile had very little effect on the increment of hinge-moment coefficient due to moving the seal from the bottom to the top position, particularly at a low angle of attack.

## Aileron Trim Characteristics

The effects of deflecting a sealed tab (fig. 3) on the aileron characteristics are shown in figures 20 to 22. The data for the aileron with cusp profile (fig. 22) were taken from previous unpublished tests of the original aileron with a sealed internal balance. The tab effectiveness at zero aileron deflection was, in general, lower and more erratic with the aileron thickened and beveled than with the original cusp contour, particularly at a low angle of attack. With the thickened and beveled aileron deflected, the tab was more effective as an unbalancing tab than as a balancing tab. Because of the differences in tab effectiveness, an airplane with beveled ailerons trimmed by means of tabs would have unsymmetrical wheel-force characteristics for right and left roll; this effect has been observed in unpublished flight tests of a fighter airplane.

Because of the erratic tab characteristics, some other device to trim thickened and beveled ailerons may be necessary. A system of trimming by springs is suggested and analyzed as follows:

A system is assumed that has a maximum aileron-control-wheel movement of $\pm 84^{\circ}$ and a control-wheel diameter of 14 inches. A maximum trimming force that can be applied in both directions equivalent to a 10-pound wheel force and a permissible increment of wheel force at full wheel deflection due to the centering action of the spring system of $2\frac{1}{2}$ pounds are assumed to be satisfactory. The spring system would consist of a single spring capable of being stressed in both directions or of two opposite springs each one-half deflected and opposing the other. One end of the spring system would be linked for suitable rotary or linear motion to a part of the aileron-control system. The other end of the spring system would be connected to an irreversible mechanism (driven by the cockpit trim control) that would deflect the spring and cause it to exert a trimming force on the aileron control system. It should be pointed out that the trimming force exerted by the spring unit, unlike that exerted by a tab, would not vary with speed. This characteristic may not be desirable. Table II is a comparison of various possible spring systems.

## Estimated Aileron-Control Characteristics

The rates of roll and the wheel forces during steady rolling were estimated for a high-speed airplane with the wing of figure 1 and table I and with the original and some of the modified ailerons. In order to be able to compare the characteristics of the various ailerons on an equal basis the maximum deflection used for each modification was that necessary to produce a $pb/2V$ of 0.09 at an indicated airspeed of 139 miles per hour. The value of $pb/2V$ of 0.09 was chosen in order to insure a suitable margin over the required minimum $pb/2V$ of 0.07. (See reference 4.) The rates of roll were estimated by means of the relationship

$$pb/2V = C_{l}'/C_{l}'_{p} \qquad (1)$$

where the coefficient of damping in roll $C_{l}'_{p}$ was taken, for the wing with the original cusp ailerons, as 0.52. This value was obtained by arbitrarily increasing the

reference 4 value 10 percent in order to account for the higher lift-curve slopes of low-drag wings. For the wing with the modified ailerons the $C_l'_p$ value of 0.52 was decreased in direct proportion to the changes in lift-curve slope due to changes in the aileron profile. (See figs. 6 to 8.) It has been assumed that the rudder will be used to counteract the yawing moment, that the aileron operating mechanism is nonelastic, and that the wing will not twist. These assumptions will result in estimated rates of roll that will be higher than would be obtained in flight with the nonrigid airplane. The wheel forces were estimated from the relationship

$$F_w = \frac{1567}{C_L}\left[ C_{h_d}\left(\frac{d\delta_a}{d\theta_w}\right)_d - C_{h_u}\left(\frac{d\delta_a}{d\theta_w}\right)_u \right] \qquad (2)$$

which may be derived from the aileron dimensions and the following airplane characteristics:

| | |
|---|---|
| Wing area, square feet | 414 |
| Span, feet | 55 |
| Taper ratio | 2.38:1 |
| Airfoil section | low-drag NACA 66 series |
| Weight, pounds | 20,561 |
| Wing loading, pounds per square foot | 49.67 |
| Wheel diameter, inches | 14 |
| Maximum wheel deflection, $\theta_w$, degrees | $\pm$84 |

The lift coefficient in equation (2) was taken from a complete airplane lift curve (fig. 23). The value of the constant in equation (2) is dependent upon the wing loading, the size of the ailerons, and the wheel diameter. For the equal up-and-down linkages, the values of $d\delta_a/d\theta_w$ were assumed constant for each arrangement and were determined from the maximum wheel deflection of $\pm 84^\circ$ and the maximum aileron deflections noted on the figures of computed results. Of the two unsymmetrically beveled ailerons, the aileron with the bevel on the top surface had more satisfactory hinge-moment characteristics for a differential linkage. A differential linkage was designed in order to take advantage of the floating tendency of this aileron. The values of $d\delta_a/d\theta_w$ for the differential linkage may be determined from figure 24. Except for two cases in which the aileron-control characteristics were computed for the static (no-roll) state, the values of $C_l'$ and $C_h$ used in equations (1) and (2) were the values computed for the steady-rolling state;

the local angle of attack at the two ailerons during rolling has been taken into account. The effective change in angle of attack over each aileron was assumed equal to the geometric change in angle at a point 1/10 of the aileron span from the inboard end of the aileron. The location of the point for determining the effective change in angle of attack was determined from comparisons of the span loadings over the aileron induced by rolling and by changing the angle of attack of the complete wing.

The estimated aileron-control characteristics at three indicated airspeeds for the airplane equipped with the original ailerons and with the various modified ailerons are presented in figure 25. Figure 26 is a comparison of the high-speed wheel forces for all the ailerons. As shown by figures 25(a), 25(b), and 26 the use of flat surfaces on the aileron did not improve the wheel-force characteristics because, for this particular model, the effect of the decrease in $\partial C_h/\partial \delta_a$ due to the flat surfaces was nearly canceled by the effect of the decrease in the negative value of $\partial C_h/\partial \alpha$ and by the fact that larger aileron deflections were necessary to attain the required value of $pb/2V$. Greater modifications to the aileron profile were more effective in reducing the wheel forces, the greatest reduction resulting from the use of the $0.20c_a$ bevel (figs. 25(a), 25(d), and 26). Using the $0.20c_a$ bevel reduced the maximum high-speed wheel force from about 150 pounds to about 40 pounds. Thickening the aileron on only the top surface gave some reduction in wheel force. The use of differential motion further reduced the wheel forces of the aileron with the $0.20c_a$ bevel on the top surface, bringing the maximum high-speed wheel force down to about 40 pounds.

The wheel forces of the original aileron and of the aileron with the $0.20c_a$ bevel are shown in figure 27 for the dynamic (steady-rolling) state and the static (no-rolling) state. For the original aileron, rolling reduced the maximum wheel force by about 9 pounds because of the negative value of $\partial C_h/\partial \alpha$. The 9-pound reduction was almost independent of speed because the negative value of $\partial C_h/\partial \alpha$ increased as the angle of attack increased. For the beveled aileron, $\partial C_h/\partial \alpha$ was positive for angles of attack of less than $8^\circ$ and therefore produced positive increments in the wheel forces at the high- and medium-speed conditions. The $0.20c_a$ bevel aileron with the top seal was the only aileron for which wheel forces were estimated that was overbalanced for the static

or no-roll state. It is not known what effect static overbalance will have on airplane handling characteristics but an analysis has indicated that, with the wheel free, there may be some oscillation of the ailerons for positive values of $\partial C_h/\partial \delta_a$ greater than about 0.001.

The changes in $\partial C_h/\partial \alpha$ and $\partial C_L/\partial \alpha$ due to thickening and beveling the aileron will cause some changes in airplane stability characteristics.

## CONCLUSIONS

The results of the tests of the 0.20-chord aileron on a tapered low-drag wing indicated that, for the arrangement tested, the following conclusions may be made:

1. Thickening and beveling the aileron trailing edge would substantially reduce the high-speed control forces.

2. Air leakage across the aileron nose tended to cause overbalance of the beveled ailerons at small deflections and to reduce their rolling-moment effectiveness. This loss in effectiveness was greater with the beveled aileron than with the original cusp aileron.

3. The characteristics of beveled ailerons were in general agreement with the characteristics obtained in previous wind-tunnel and flight tests. A comparison of the results of the present and previous tests indicated that the included angle between the upper and lower surfaces at the trailing edge is a convenient basis for correlation of the hinge-moment characteristics. The changes in the slope of the curves of hinge-moment and lift coefficient with respect to angle of attack (due to thickening and beveling the aileron) will cause some changes in airplane stability characteristics.

4. Thickening and beveling only one surface of the aileron gave less aerodynamic balance than thickening and beveling both surfaces and produced a large floating tendency that would allow advantageous use of a differential aileron linkage.

5. Tab effectiveness varied with aileron profile and in some cases was unsatisfactory.

Langley Memorial Aeronautical Laboratory,
National Advisory Committee for Aeronautics,
Langley Field, Va.

## REFERENCES

1. Jones, Robert T., and Ames, Milton, B., Jr.: Wind-Tunnel Investigation of Control-Surface Characteristics. V - The Use of a Beveled Trailing Edge to Reduce the Hinge Moment of a Control Surface. NACA A.R.R., March 1942.

2. Rogallo, F. M., and Purser, Paul E.: Wind-Tunnel Investigation of a Plain Aileron with Various Trailing-Edge Modifications on a Tapered Wing. II - Ailerons with Thickened and Beveled Trailing Edges. NACA A.R.R., Oct. 1942.

3. Wenzinger, Carl J., and Harris, Thomas A.: Wind-Tunnel Investigation of an N.A.C.A. 23012 Airfoil with Various Arrangements of Slotted Flaps. Rep. No. 664, NACA, 1939.

4. Gilruth, R. R., and Turner, W. N.: Lateral Control Required for Satisfactory Flying Qualities Based on Flight Tests of Numerous Airplanes. Rep. No. 715, NACA, 1941.

TABLE I

GEOMETRIC CHARACTERISTICS OF LOW-DRAG WING AND 0.40-SCALE MODEL

| Wing | Wing area (sq ft) | Partial-span wing area (sq ft) | Wing span (in.) | Root chord (in.) | Tip chord (in.) | M.A.C. (in.) | Aspect ratio |
|---|---|---|---|---|---|---|---|
| Full size | 414 | 118.6 | 660 | 128.00 | 53.85 | 96.33 | 7.3 |
| 0.40-scale model | 66.24 | 18.98 | 264 | 51.20 | 21.54 | 38.53 | 7.3 |
| 0.40-scale model partial-span | -------- | 18.98 | ------ | 41.33 | 21.54 | -------- | ---------- |

| Wing | Aileron root-mean-square chord (in.) | Aileron area (one aileron) (sq in.) | Aileron chord inboard hinge (in.) | Aileron chord, outboard hinge (in.) | NACA airfoil section at station 110 (model station, 0) | NACA airfoil section at station 308 (model station, 79.2) |
|---|---|---|---|---|---|---|
| Full size | 14.44 | 2200 | 17.78 | 11.60 | 66,2-2(13.716) | 66,2-2(13.125) |
| 0.40-scale model | 5.78 | 352 | 7.11 | 4.64 | 66,2-2(13.716) | 66,2-2(13.125) |
| 0.40-scale model partial-span | 5.78 | 352 | 7.11 | 4.64 | 66,2-2(13.716) | 66,2-2(13.125) |

TABLE II

CHARACTERISTICS OF SPRING TRIMMING SYSTEMS

| Type of spring system | Theoretical spring efficiency (percent) | Practical spring efficiency (percent) | Type of stress | Modulus of elasticity (lb/sq in.) | Maximum allowable stress (lb/sq in.) |
|---|---|---|---|---|---|
| Tension-compression bar | 100 | Unusable | Tension-compression | 30,000,000 | 130,000 |
| Opposed flat coil (clock type) | 33.3 | 30.0 | Bending | 30,000,000 | 130,000 |
| Opposed torsion (circular wire, D/d = 10)[a] | 21.4 | 21.4 | Bending | 30,000,000 | 130,000 |
| Torsion bar (circular) | 50.0 | 50.0 | Shear | 11,500,000 | 50,000 |
| Compression-tension (circular wire, D/d = 10)[a] | 38.5 | 38.5 | Shear | 11,500,000 | 50,000 |

| Type of spring system | Number of springs required | Total weight of active spring material (lb) | Approximate size of each spring (in.) | Spring deflection from neutral at full trim | Spring deflection from neutral due to full wheel movement |
|---|---|---|---|---|---|
| Tension-compression bar | 1 | 0.32 | ---------- | ---------- | ---------- |
| Opposed flat coil (clock type) | 2 | 4.29 | $\frac{1}{16}$ × 1 steel<br>O.D., 4.94<br>I.D., 2 | 386° | 96.6° |
| Opposed torsion (circular wire, D/d = 10)[a] | 2 | 6.02 | 1/4 wire<br>O.D., 2.75<br>Length, 6.90 | 692° | 173.0° |
| Torsion bar (circular) | 1 | 1.67 | Diam., $\frac{3}{8}$<br>Length, 53.3 | 56.8° | 14.2° |
| Compression-tension (circular wire, D/d = 10)[a] | 1 | 2.17 | 1/4 wire<br>O.D., 2.75<br>Free length, 11.7 | 5.4 in. | 1.35 in. |

[a]D, mean diameter of coil; d, diameter of wire.

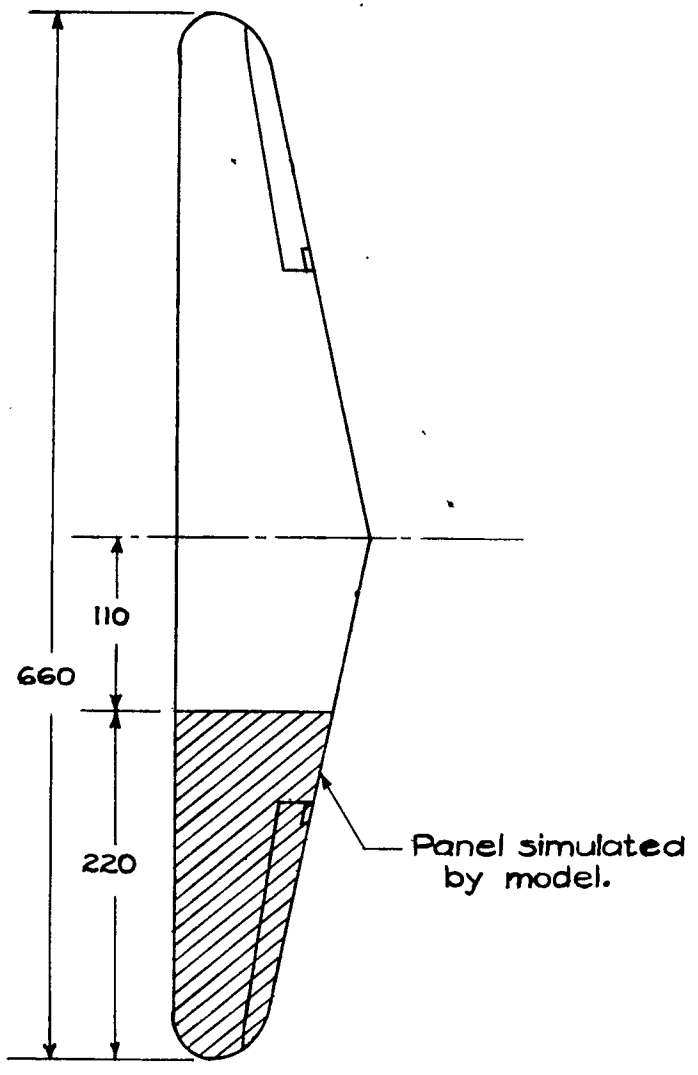


FIGURE 1.- Plan form of low-drag wing.

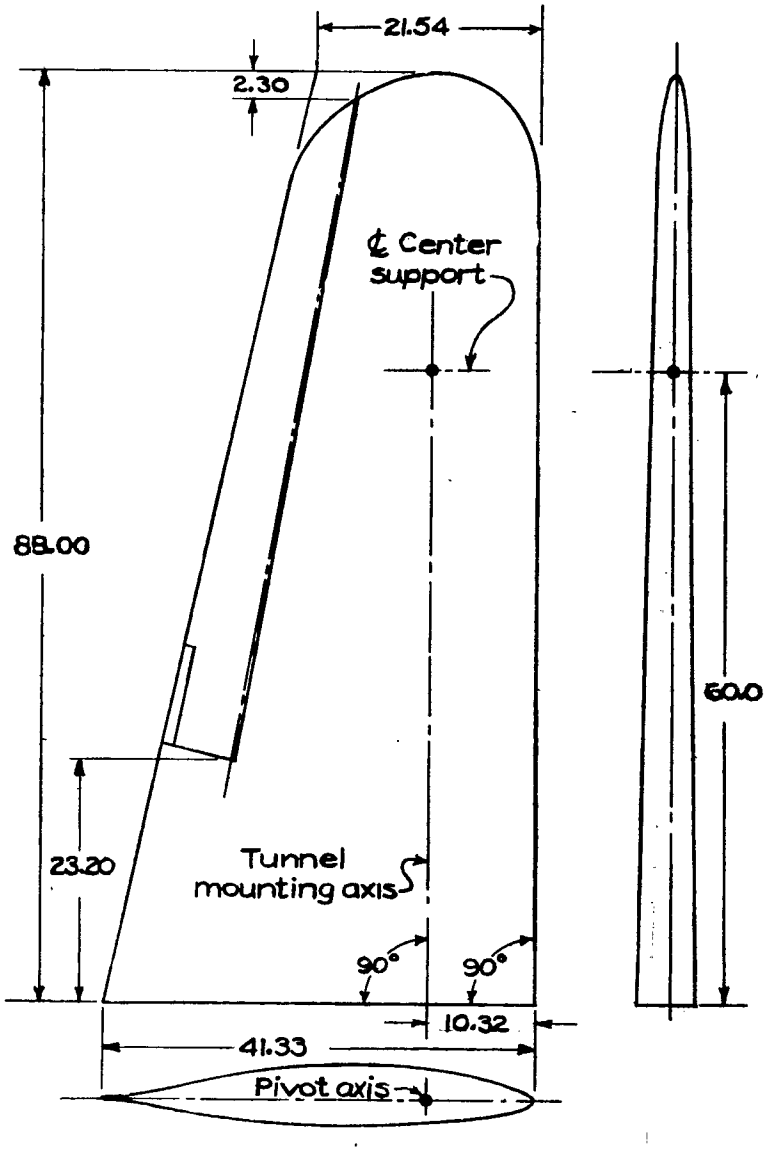


FIGURE 2.- 0.40-scale partial-span model of low-drag wing.

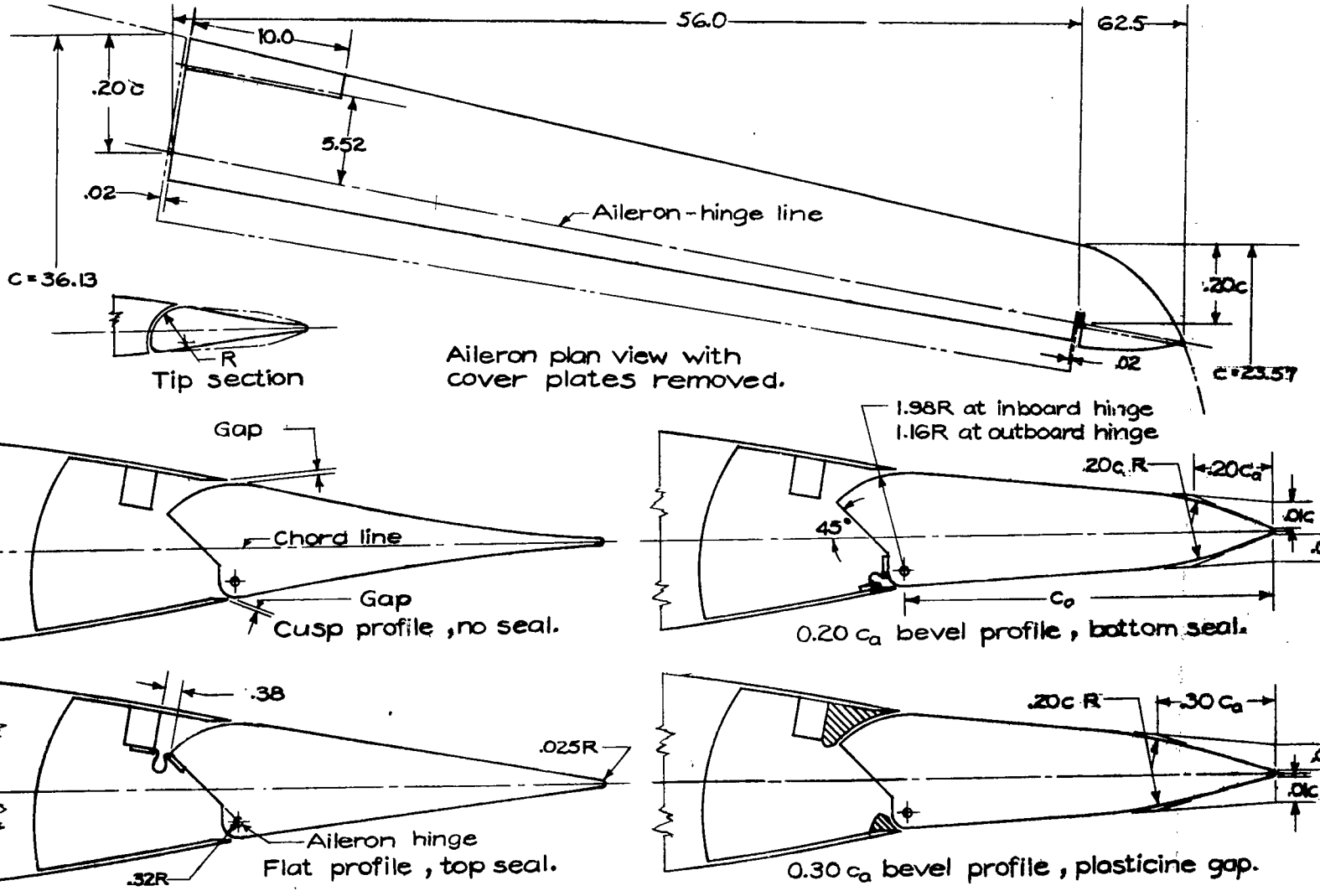


FIGURE 3.- Aileron with typical profile modifications tested on 0.40-scale partial-span model of a low-drag wing.

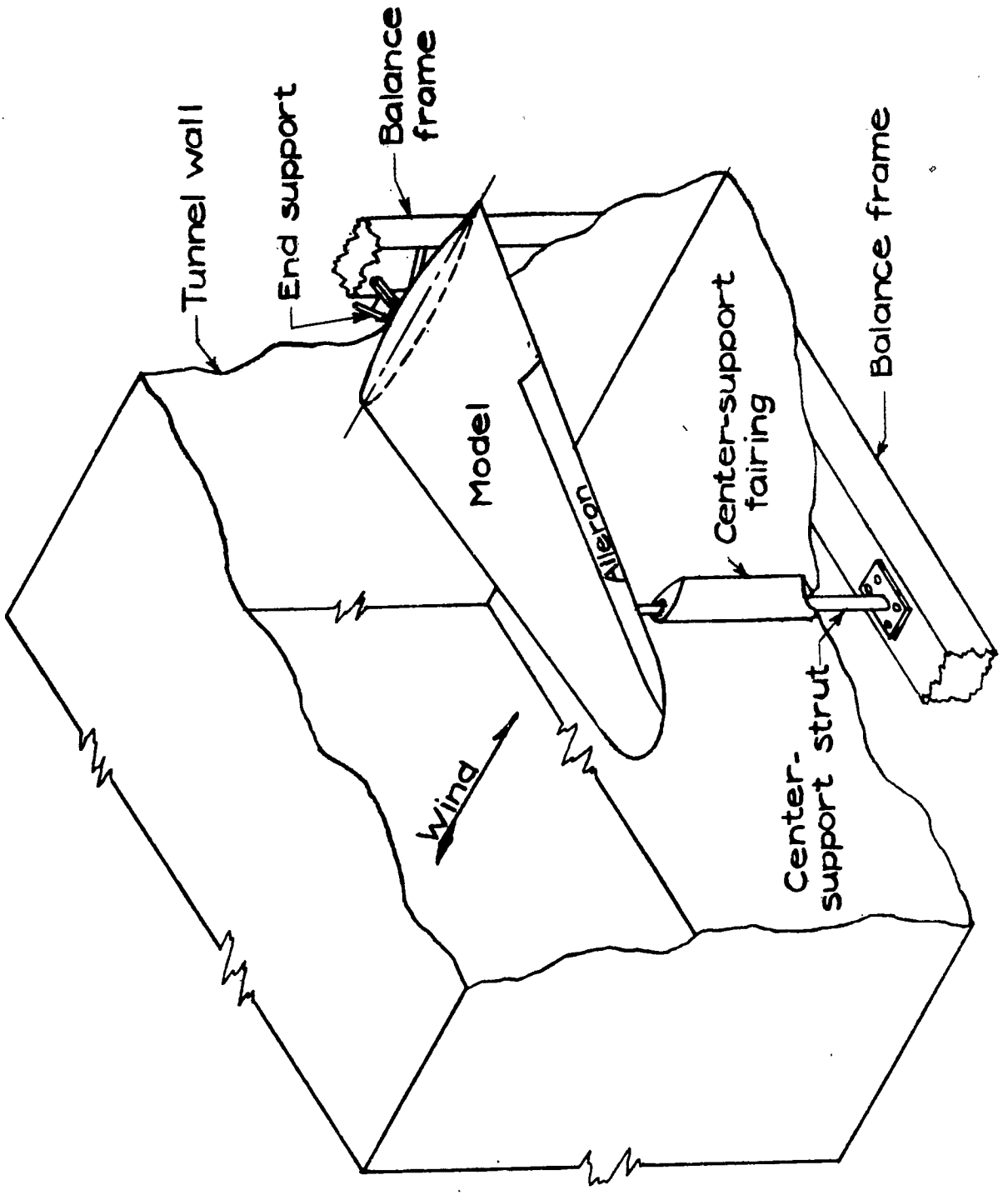


FIGURE 4.- Schematic diagram of test installation.

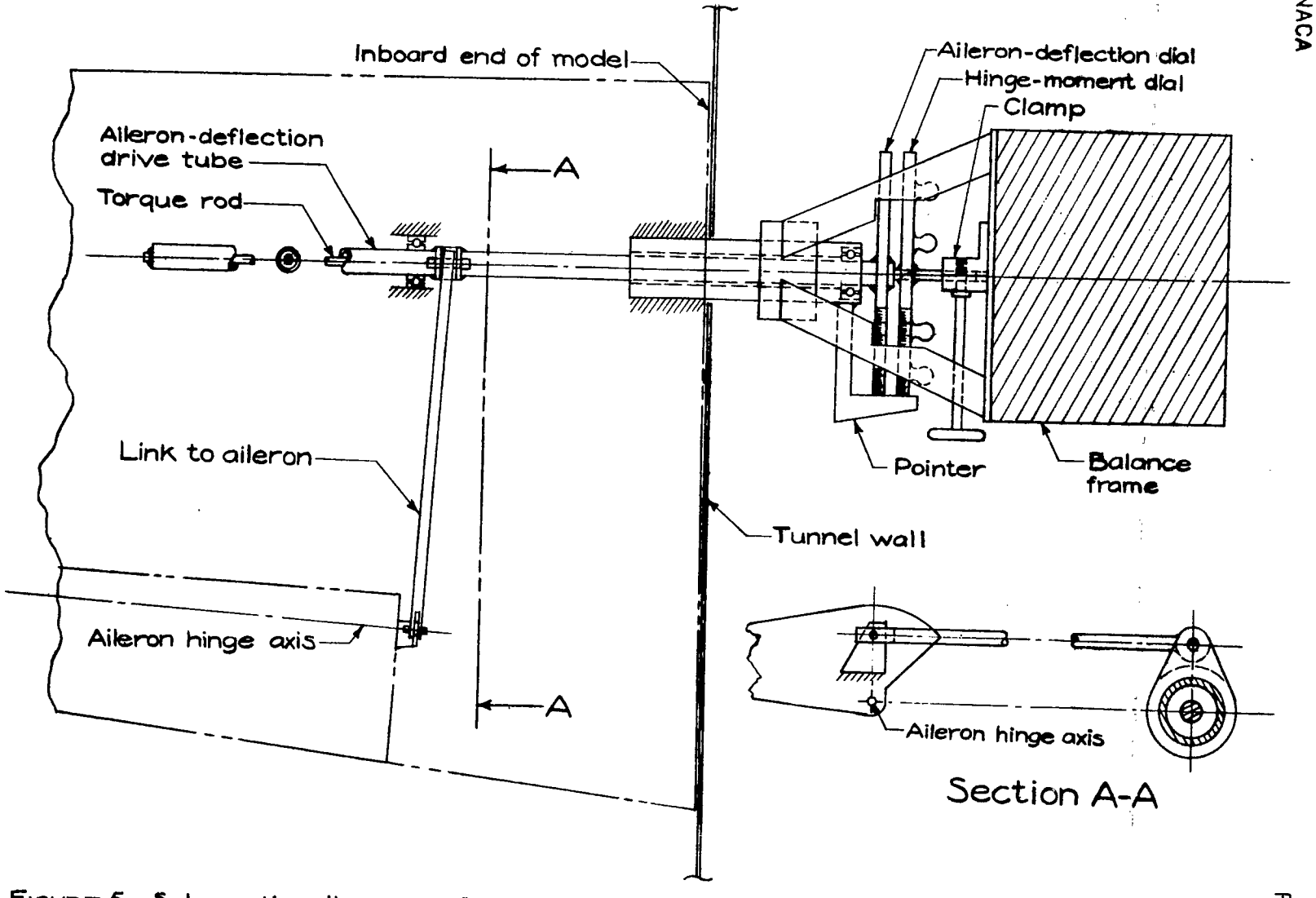


FIGURE 5.- Schematic diagram of aileron hinge-moment and deflection device.

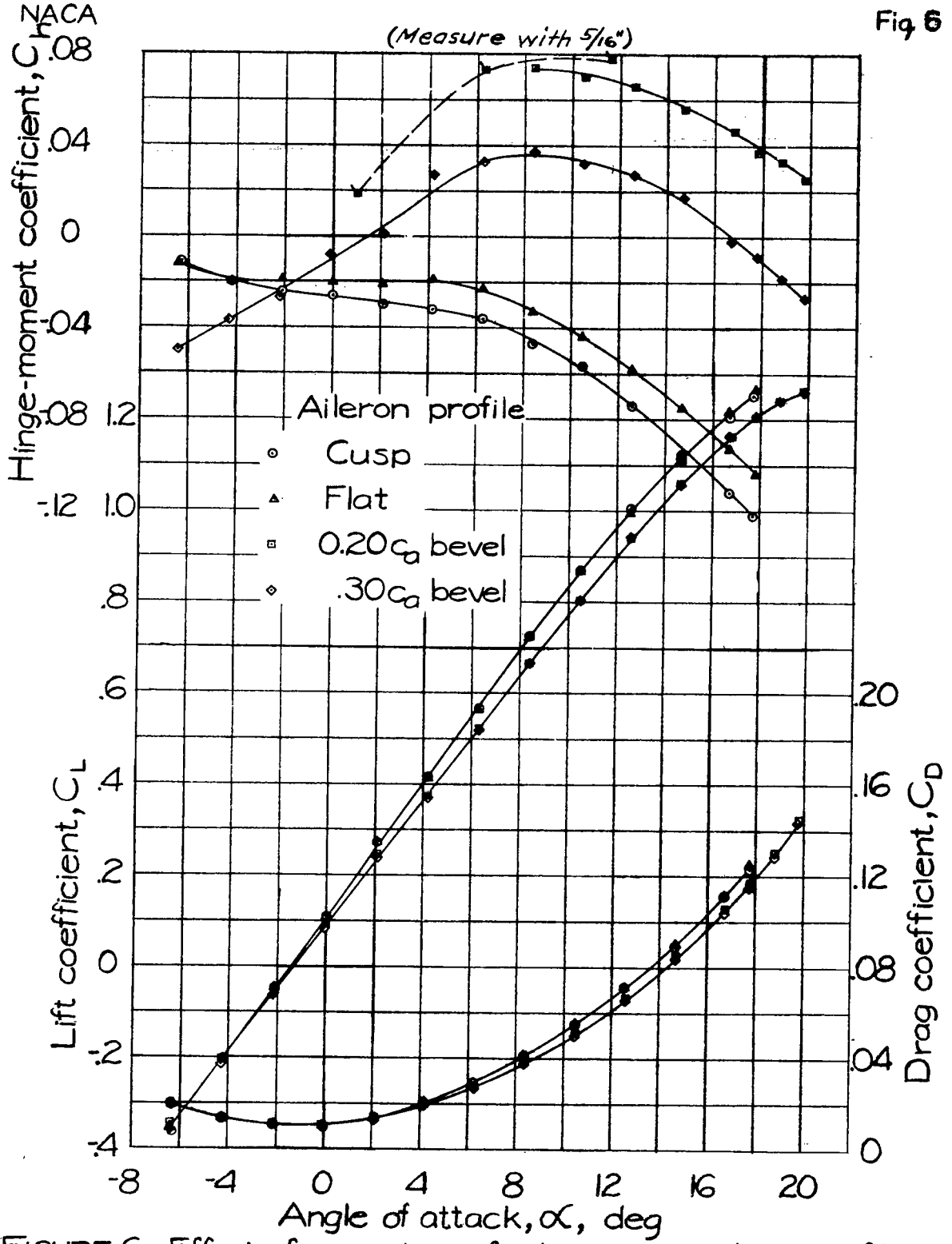


FIGURE 6.- Effect of several modifications of the aileron profile on the aerodynamic characteristics of the 0.40-scale model of a low-drag wing; no seal; 0.004c gaps; $\delta_a = 0$.

NACA

Fig. 7

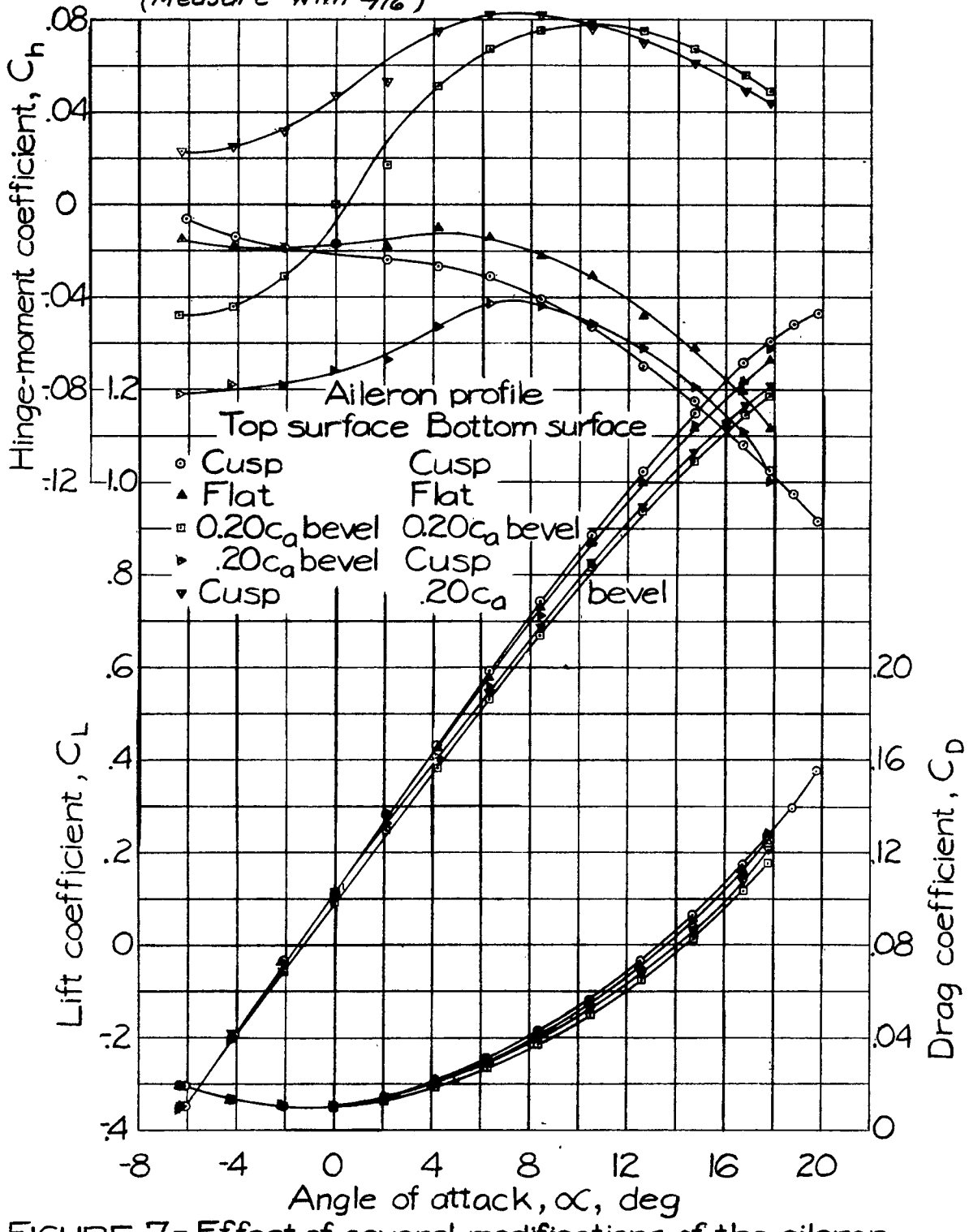


FIGURE 7.- Effect of several modifications of the aileron profile on the aerodynamic characteristics of the 0.40-scale model of a low-drag wing; top seal; 0.004c gaps; $\delta_a = 0$.

NACA

Fig. 8

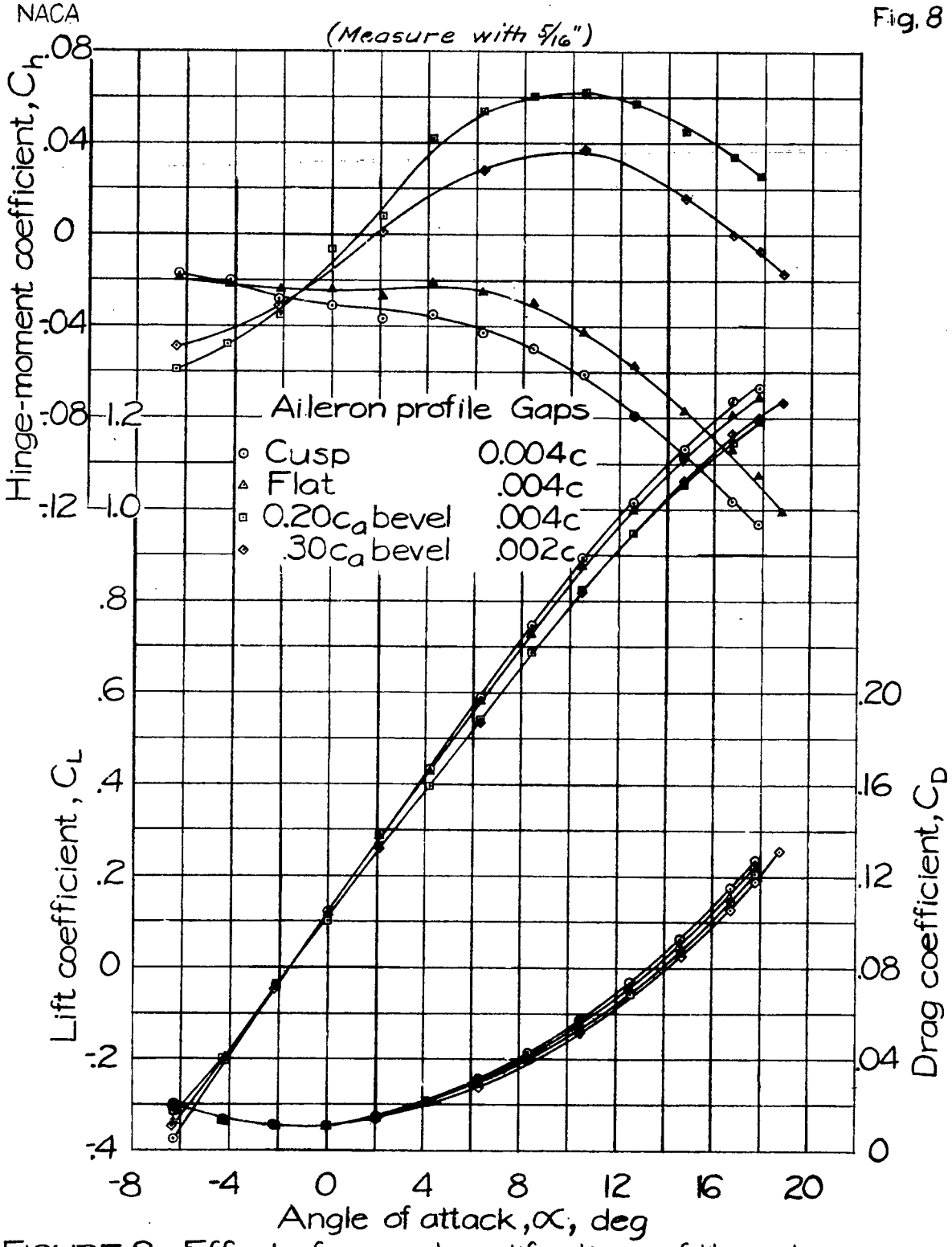


FIGURE 8.- Effect of several modifications of the aileron profile on the aerodynamic characteristics of the 0.40-scale model of a low-drag wing ; bottom seal; $\delta_a$=0.

NACA

Fig. 9

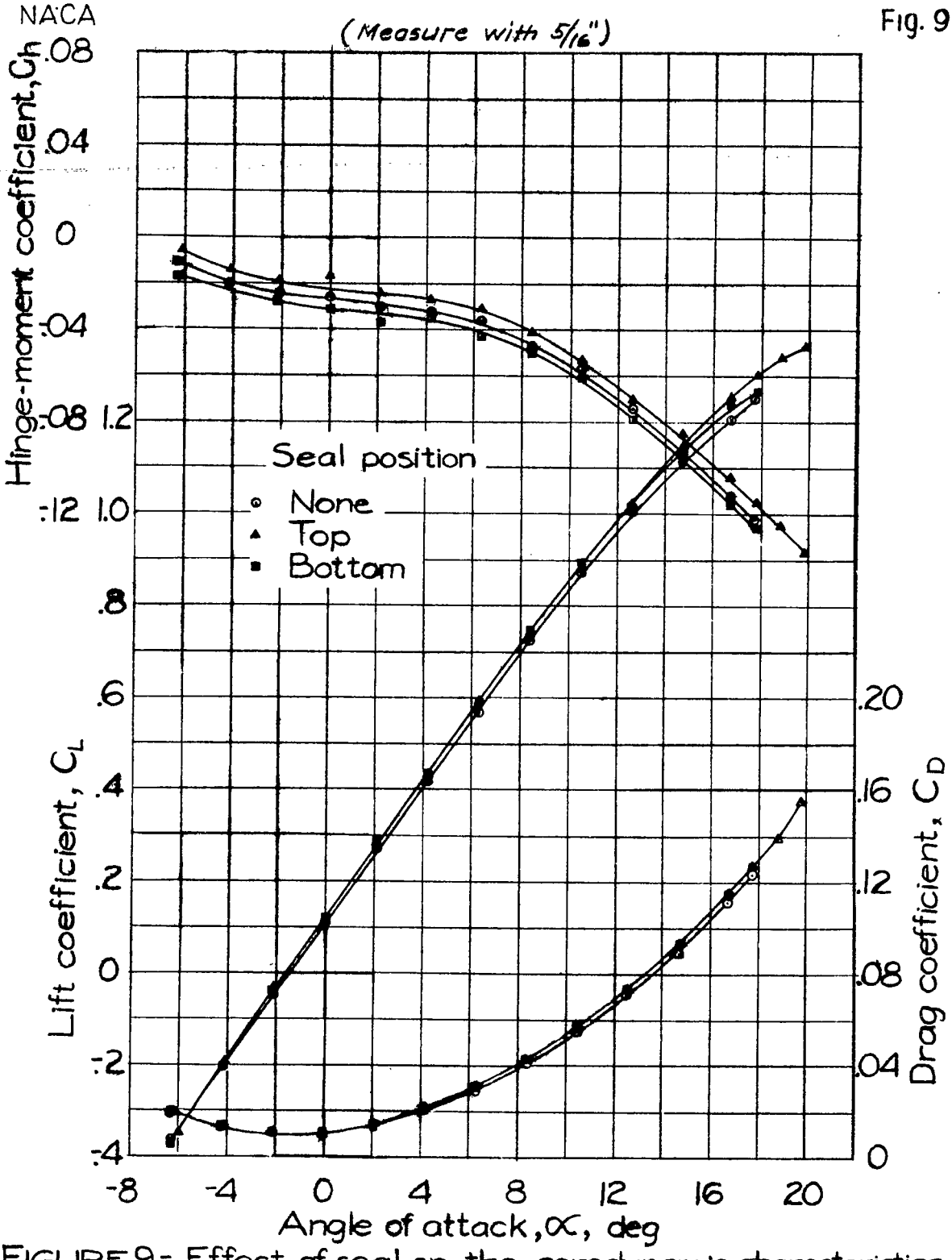


FIGURE 9.- Effect of seal on the aerodynamic characteristics of the 0.40-scale model of a low-drag wing; cusp aileron profile; 0.004c gaps; $\delta_a = 0$.

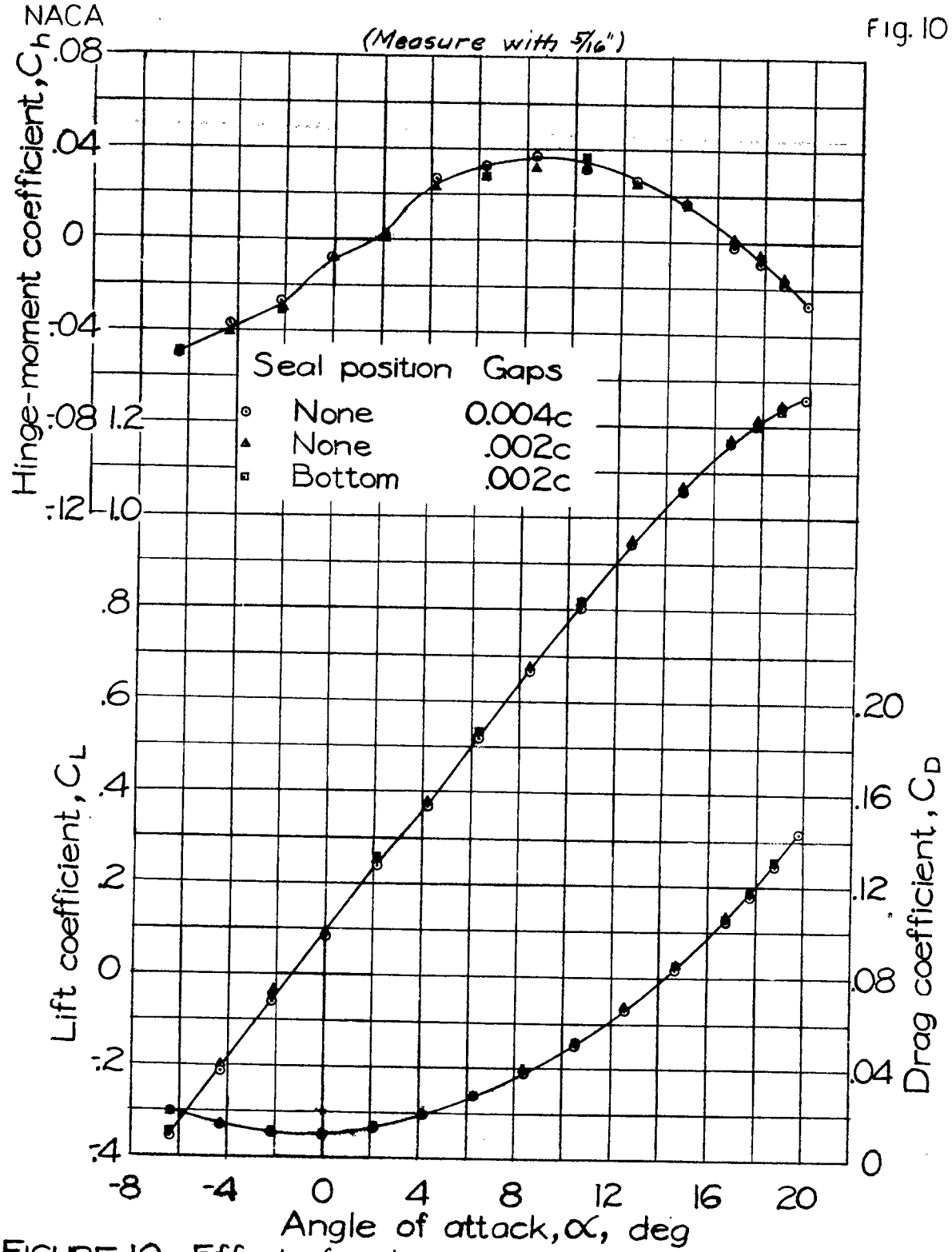


FIGURE 10.- Effect of seal and gap on the aerodynamic characteristics of the 0.40-scale model of a low-drag wing; 0.30 $c_a$ bevel aileron profile; $\delta_a = 0$.

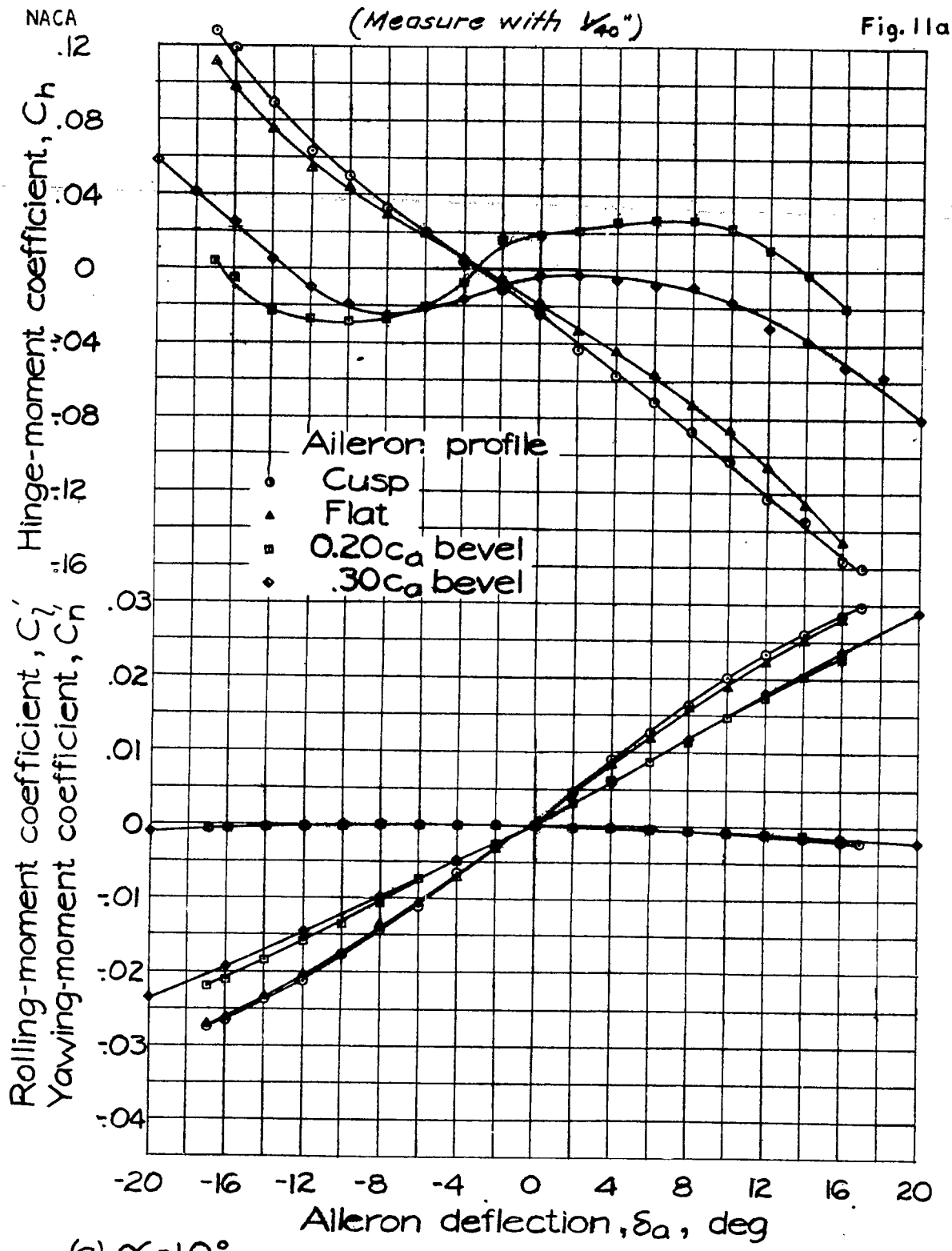


(a) $\alpha = 1.0°$.

FIGURE 11.- Effect of several modifications of the aileron profile on the aileron characteristics of the 0.40-scale model of a low-drag wing; no seal; 0.004c gaps.

NACA

(Measure with 1/40")

Fig. 11b

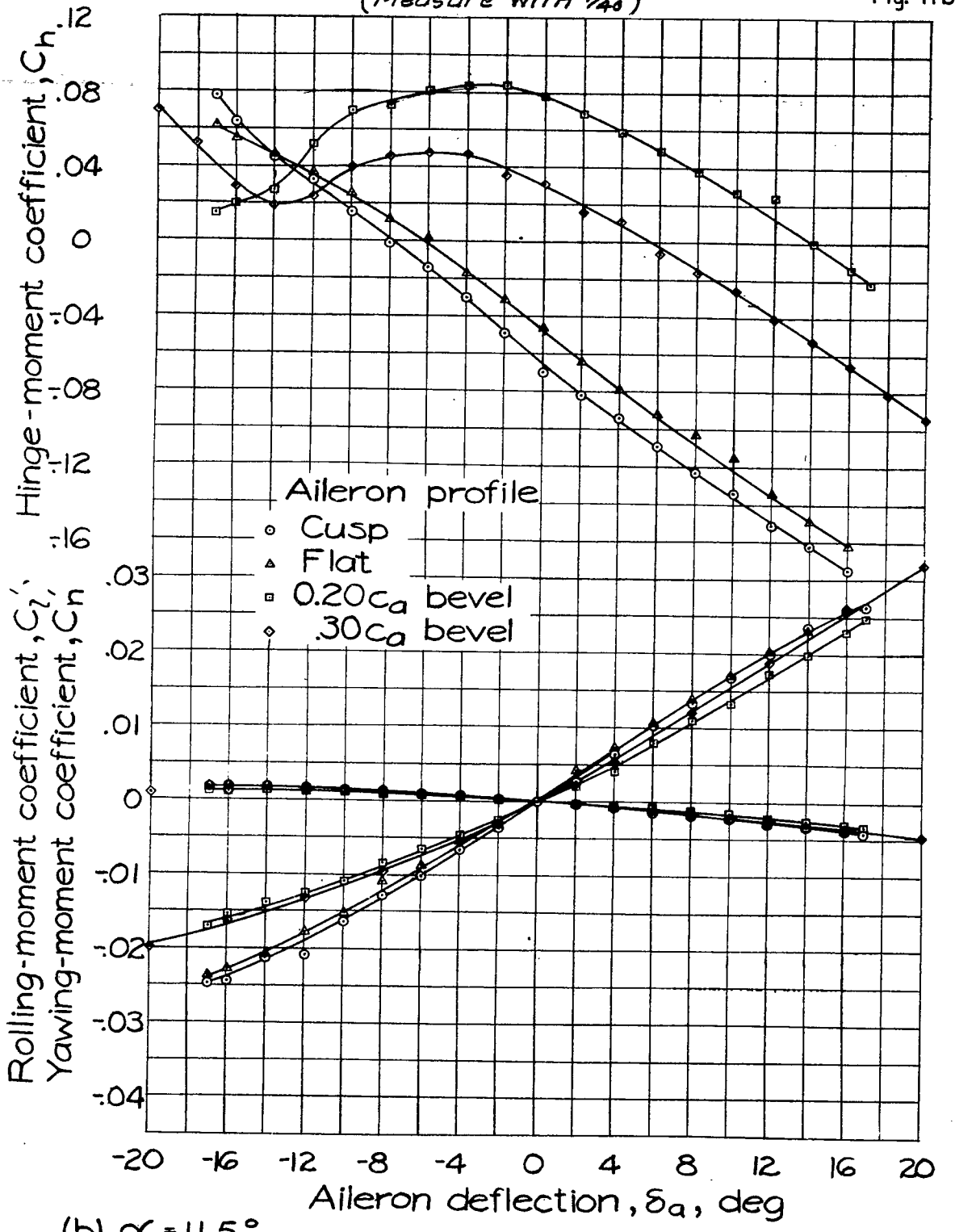


(b) $\alpha = 11.5°$

FIGURE 11.- Concluded.

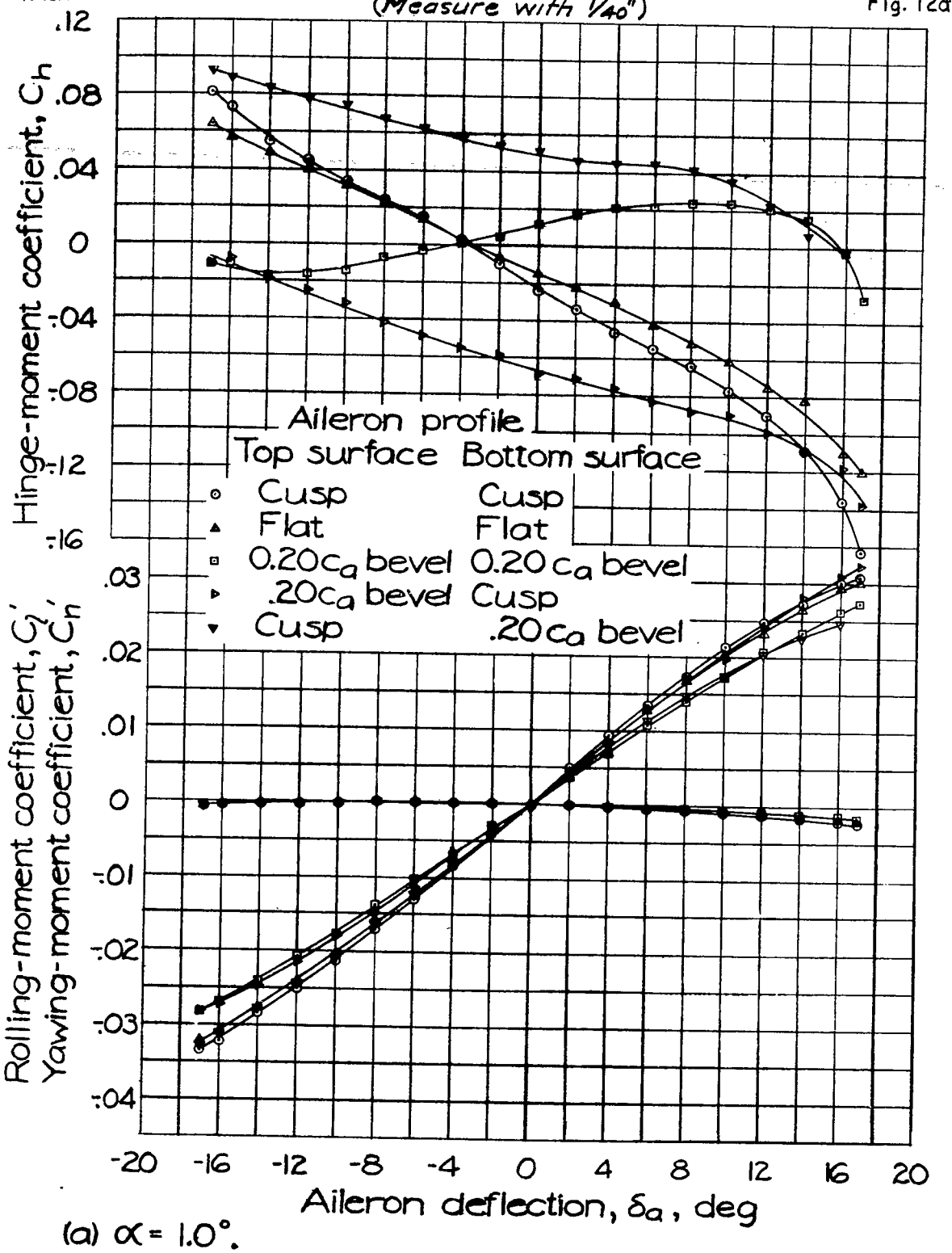


(a) $\alpha = 1.0°$.

FIGURE 12.- Effect of several modifications of the aileron profile on the aileron characteristics of the 0.40-scale model of a low-drag wing; top seal; 0.004c gaps.

NACA

(Measure with 1/40")

Fig. 12b

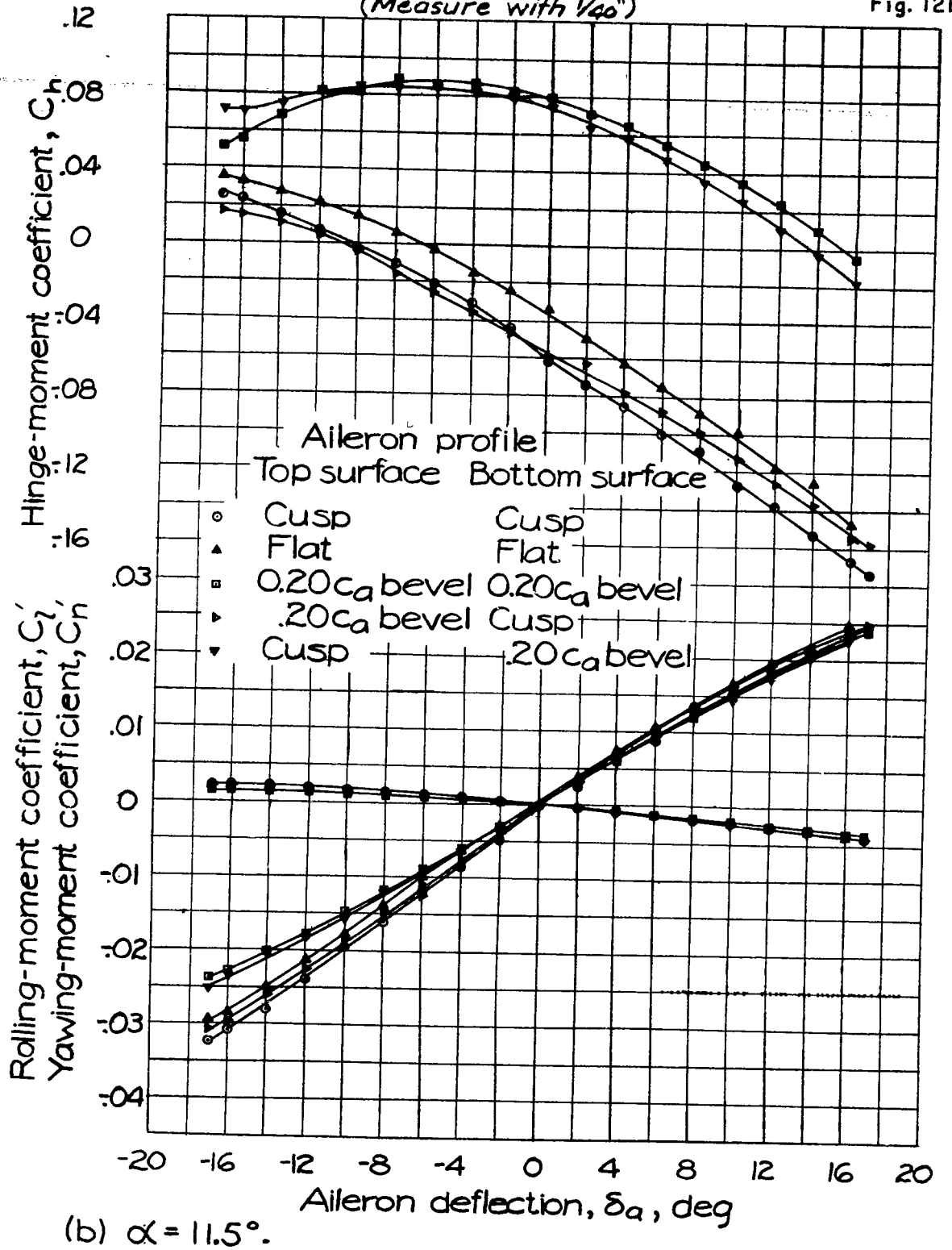


(b) $\alpha = 11.5°$.

FIGURE 12.- Concluded.

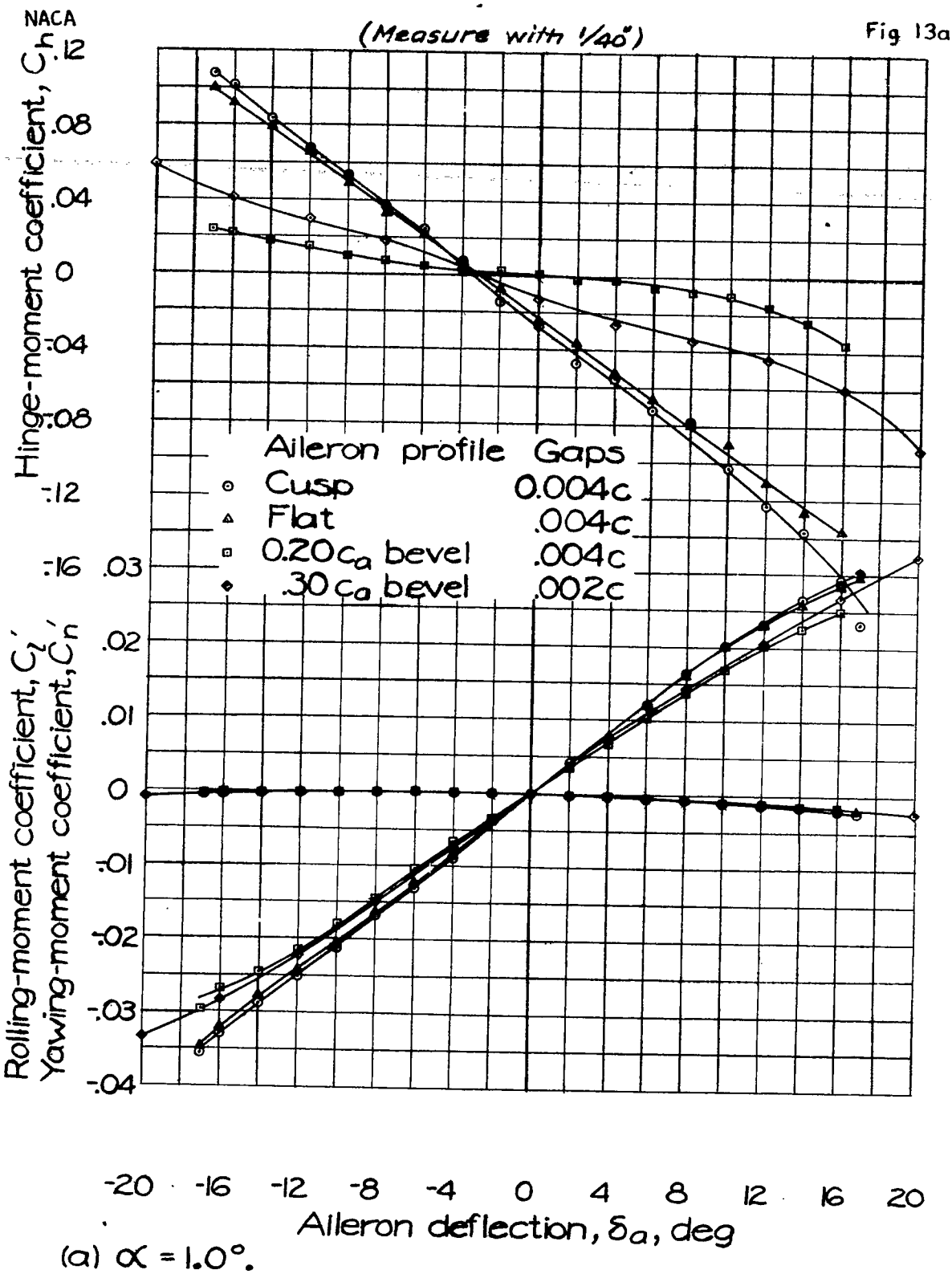


(a) $\alpha = 1.0°$.

FIGURE 13.- Effect of several modifications of the aileron profile on the aileron characteristics of the 0.40-scale model of a low-drag wing; bottom seal.

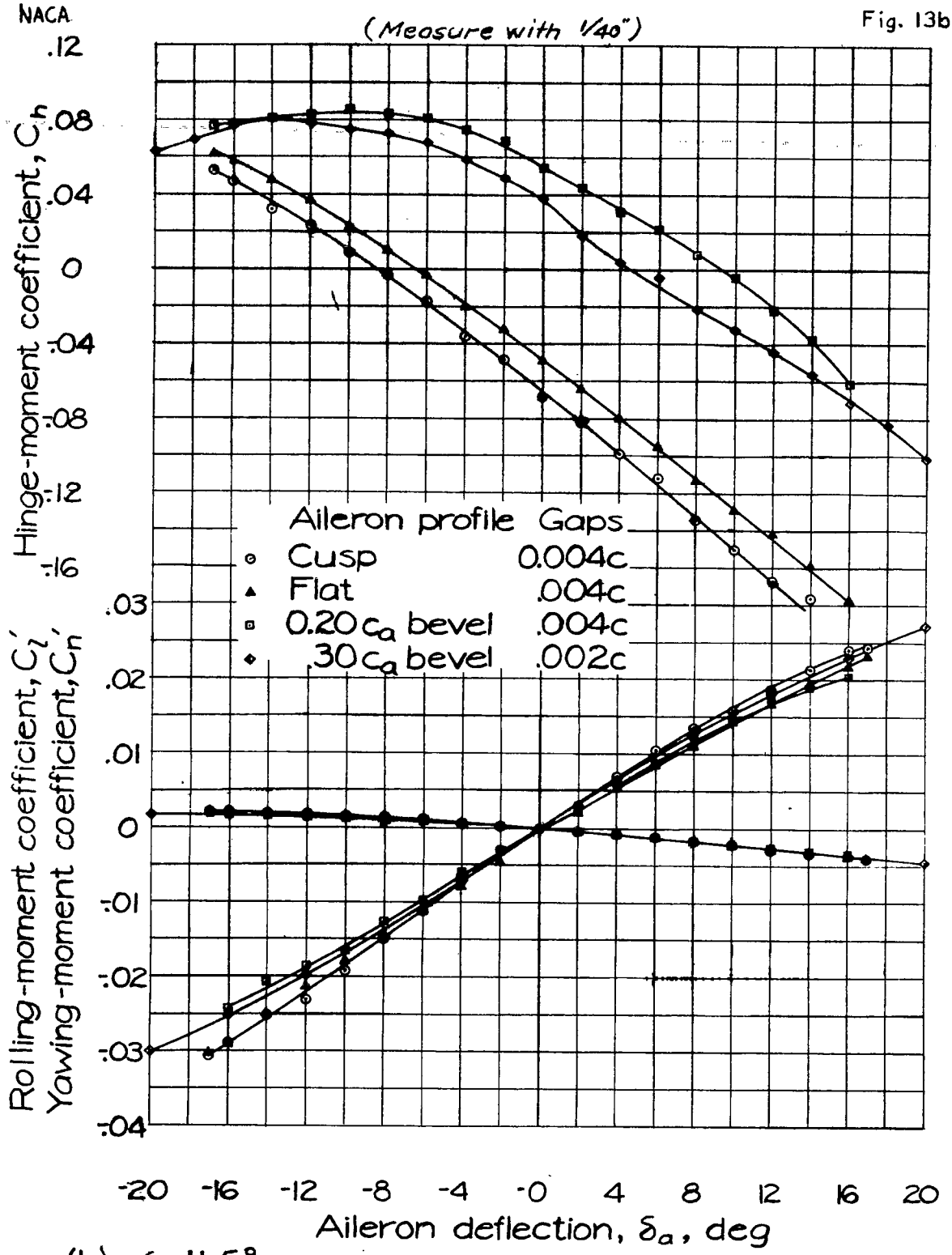


(b) $\alpha = 11.5°$.

FIGURE 13.-Concluded.

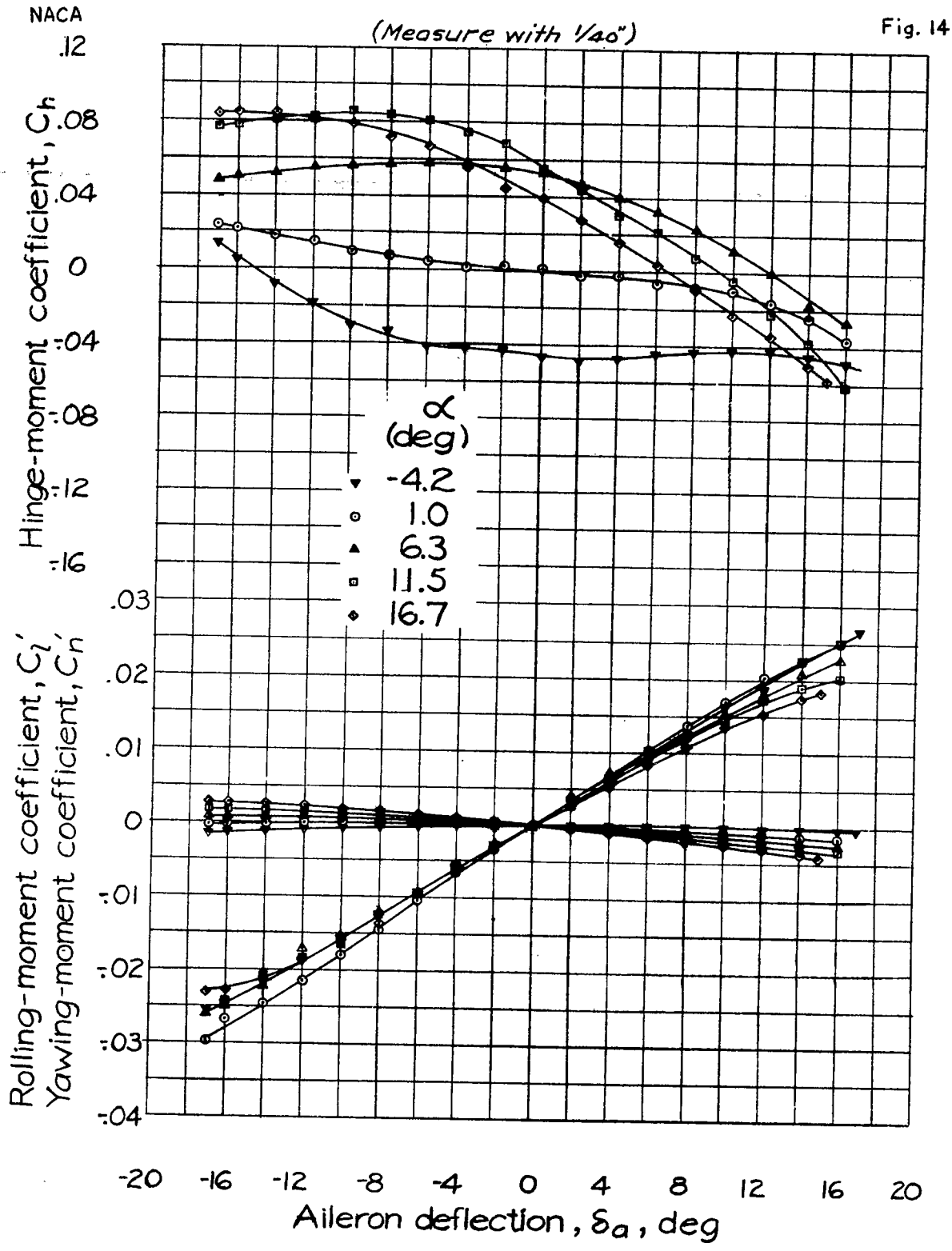


FIGURE 14.- Aileron characteristics of the 0.40-scale model of a low-drag wing; $0.20c_a$ bevel aileron profile; bottom seal; 0.004c gaps.

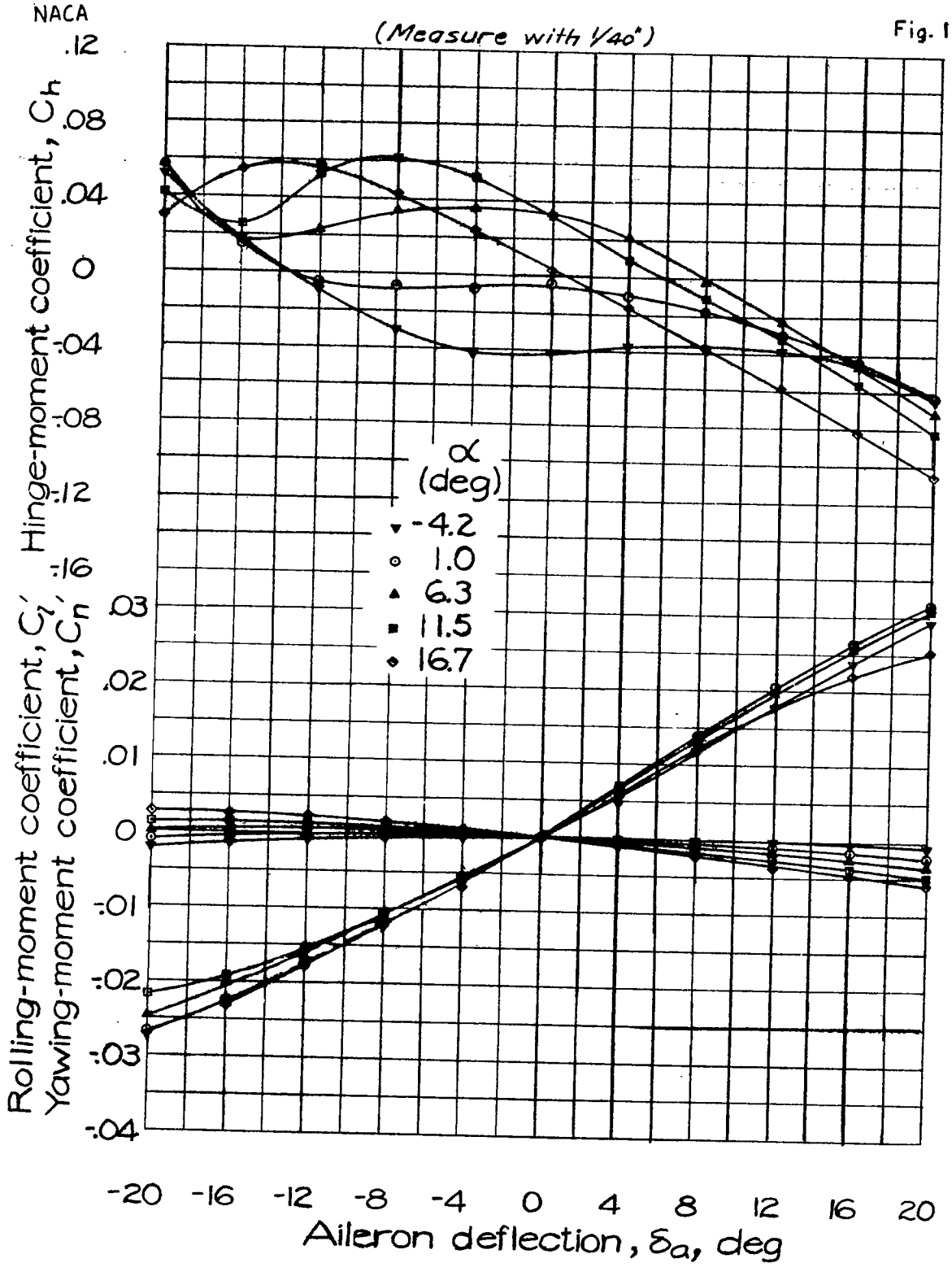


FIGURE 15.- Aileron characteristics of the 0.40-scale model of a low-drag wing; 0.30$c_a$ bevel aileron profile; no seal; 0.002c gaps.

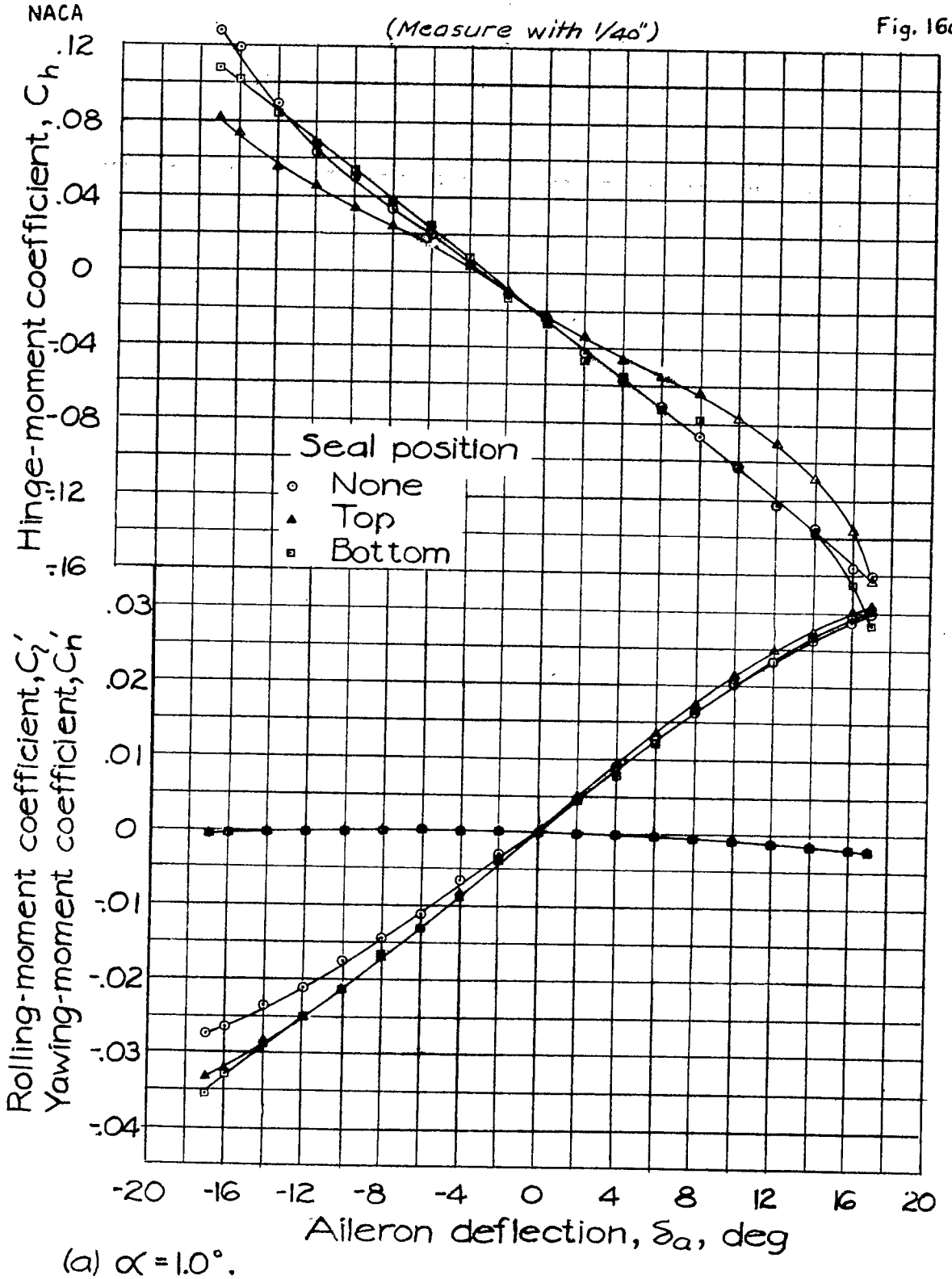


(a) $\alpha = 1.0°$.

FIGURE 16.- Effect of seal on the aileron characteristics of the 0.40-scale model of a low-drag wing; cusp aileron profile; 0.004c gaps.

NACA

(Measure with 1/40")

Fig. 16b

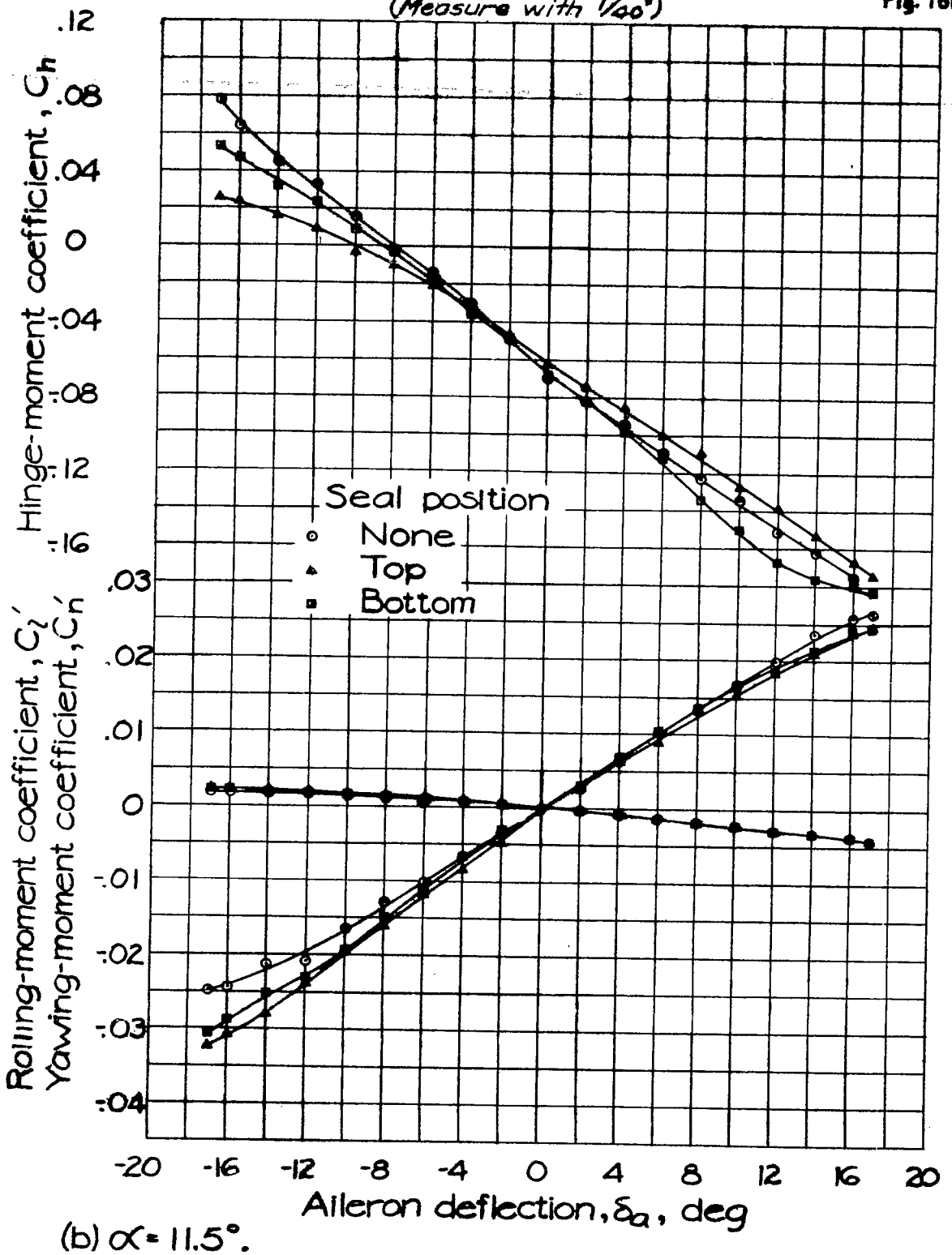


(b) $\alpha = 11.5°$.

FIGURE 16.- Concluded.

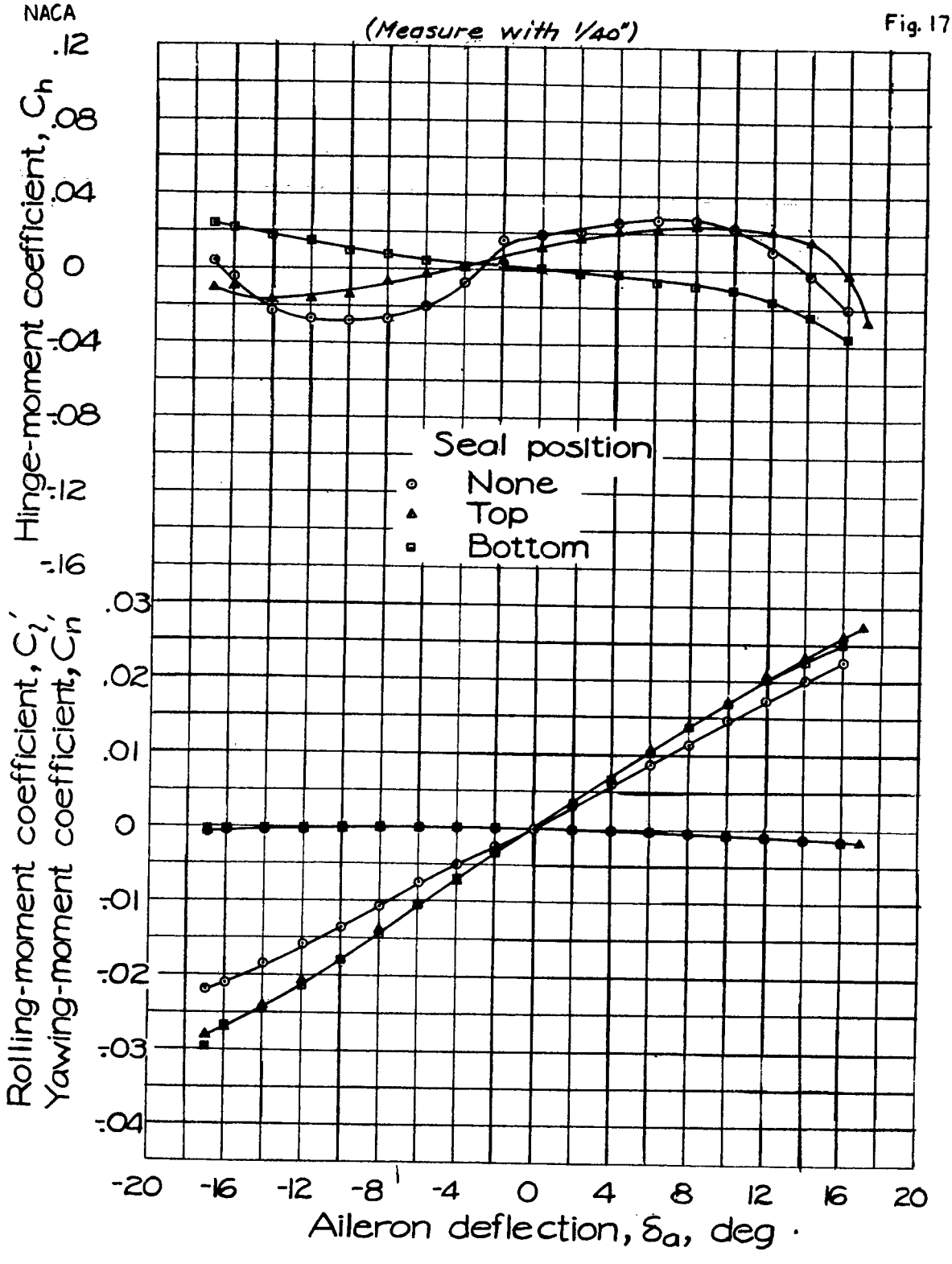


FIGURE 17.- Effect of seal on the aileron characteristics of the 0.40-scale model of a low-drag wing; 0.20 $c_a$ bevel aileron profile; 0.004c gaps; $\alpha = 1.0°$.

(Measure with 1/40")



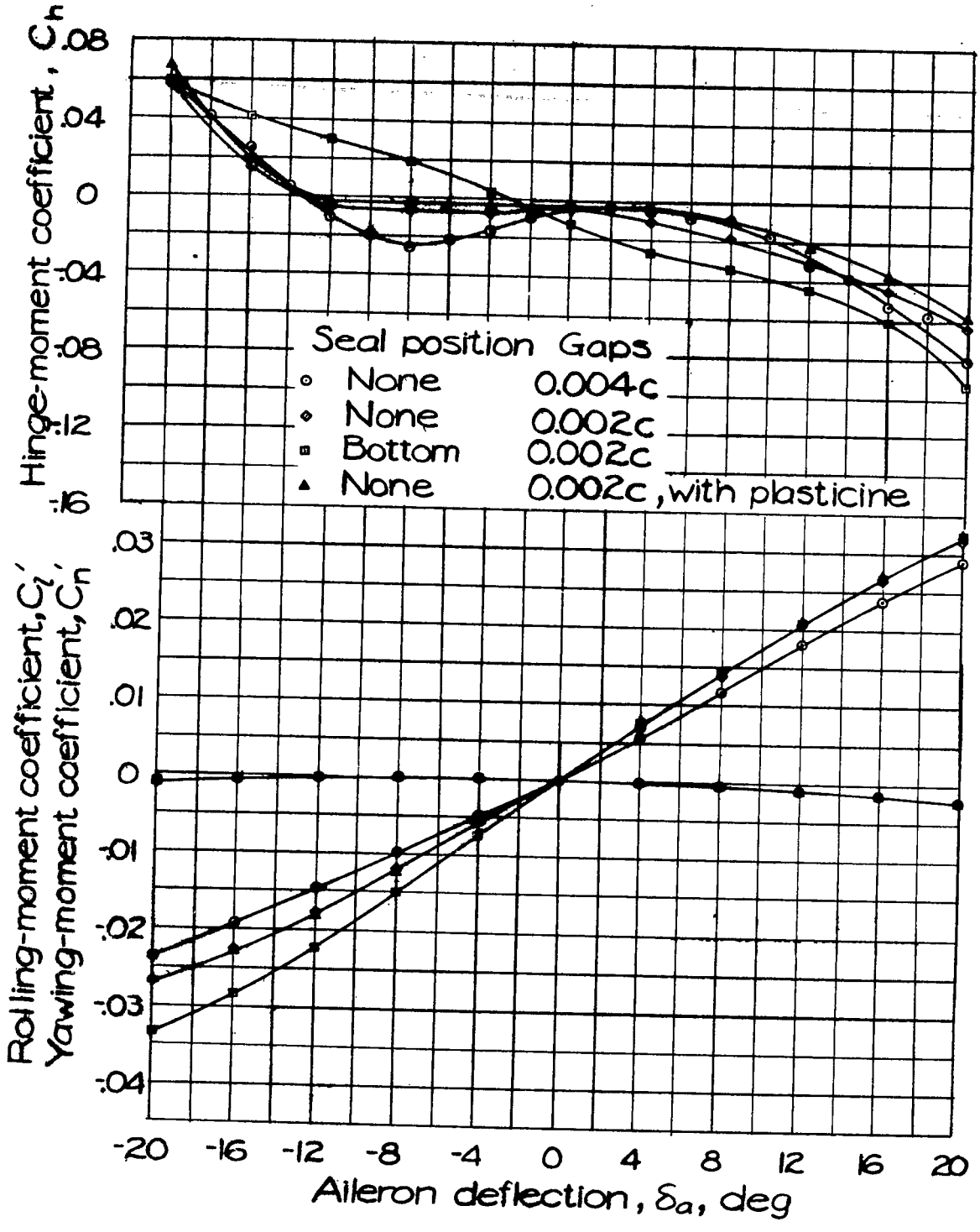


FIGURE 18: Effect of seal and gap on the aileron characteristics of the 0.40-scale model of a low-drag wing; $0.30c_a$ bevel aileron profile; $\alpha = 1.0°$.

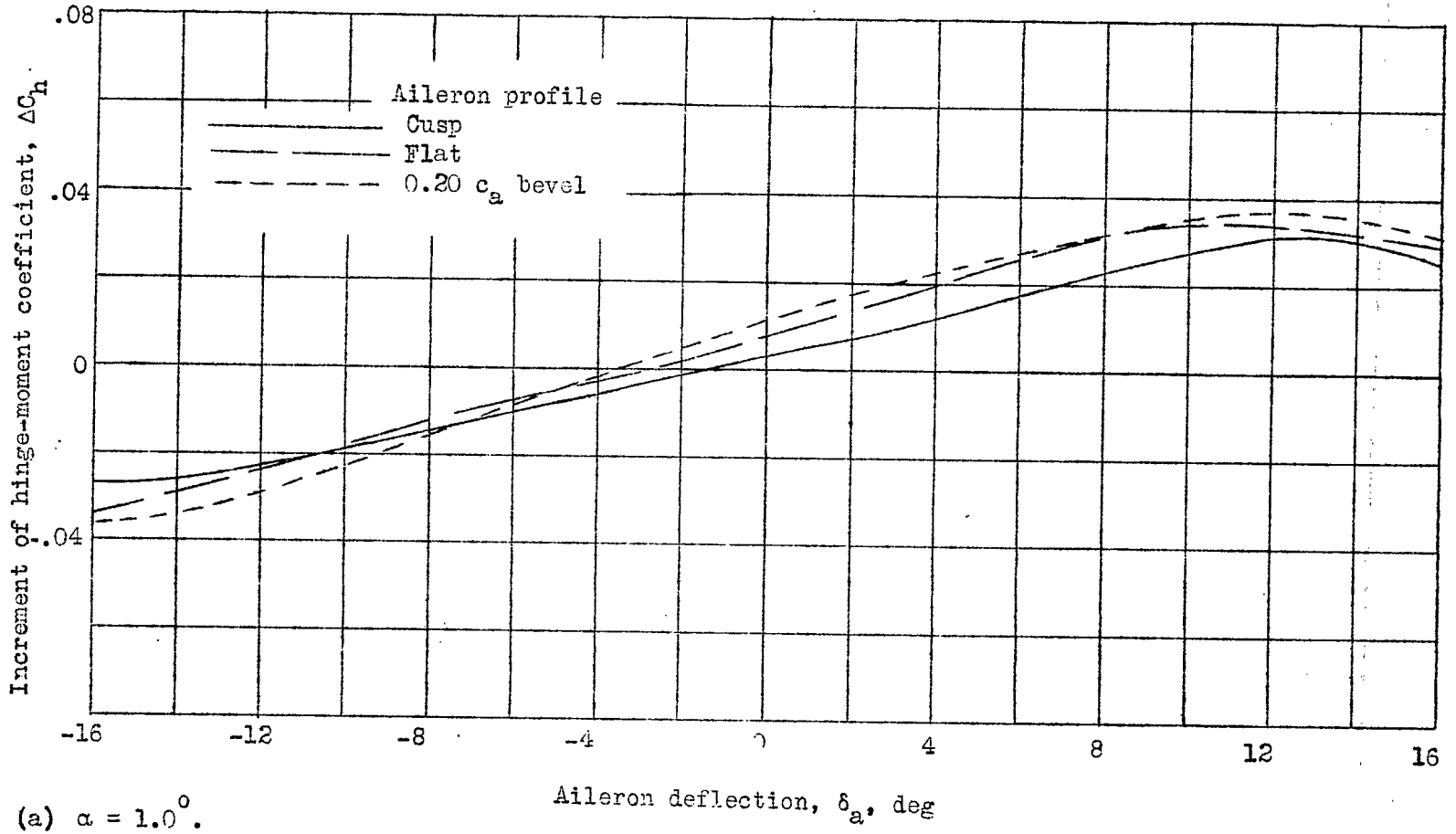


(a) $\alpha = 1.0^\circ$.

Figure 19a, b.- Increment of hinge-moment coefficient $\Delta C_h$ caused by moving the seal from the bottom to the top position.

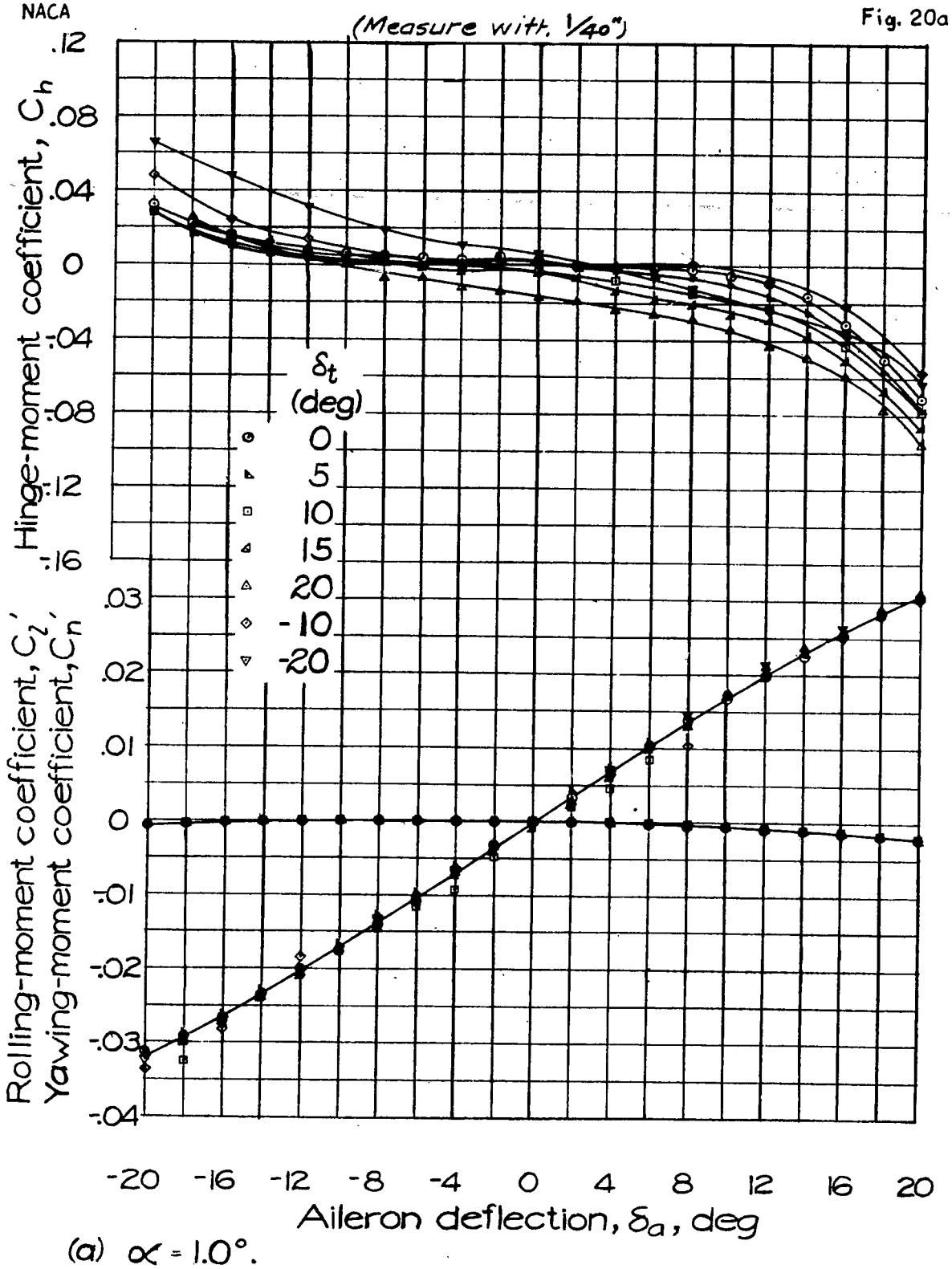


(a) $\alpha = 1.0°$.

FIGURE 20.- Effect of tab deflection on the aileron characteristics of the 0.40-scale model of a low-drag wing; $0.20c_a$ bevel aileron profile; bottom seal; 0.004c gaps.

NACA (Measure with 1/40") Fig. 20b

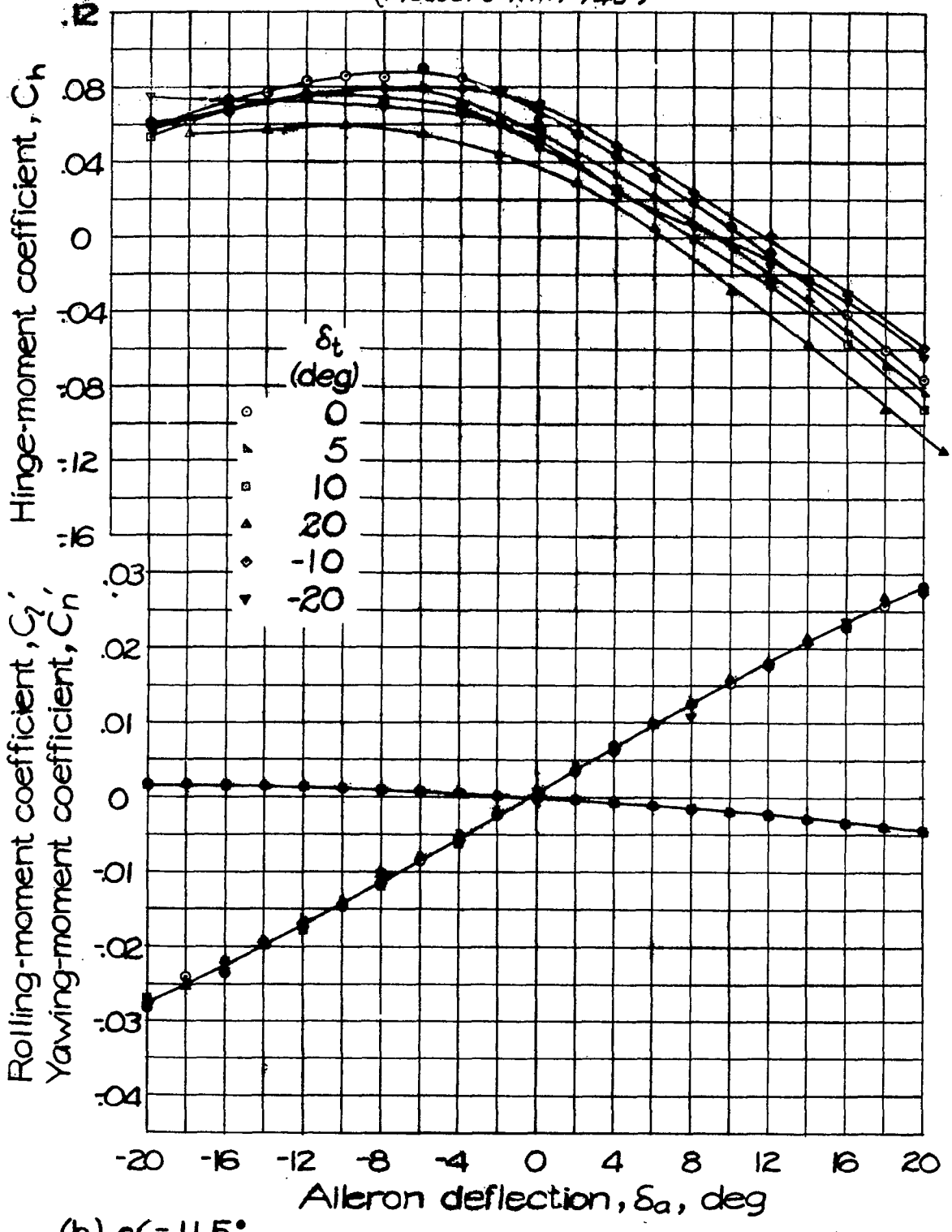


(b) $\alpha = 11.5°$.

FIGURE 20.-Concluded.

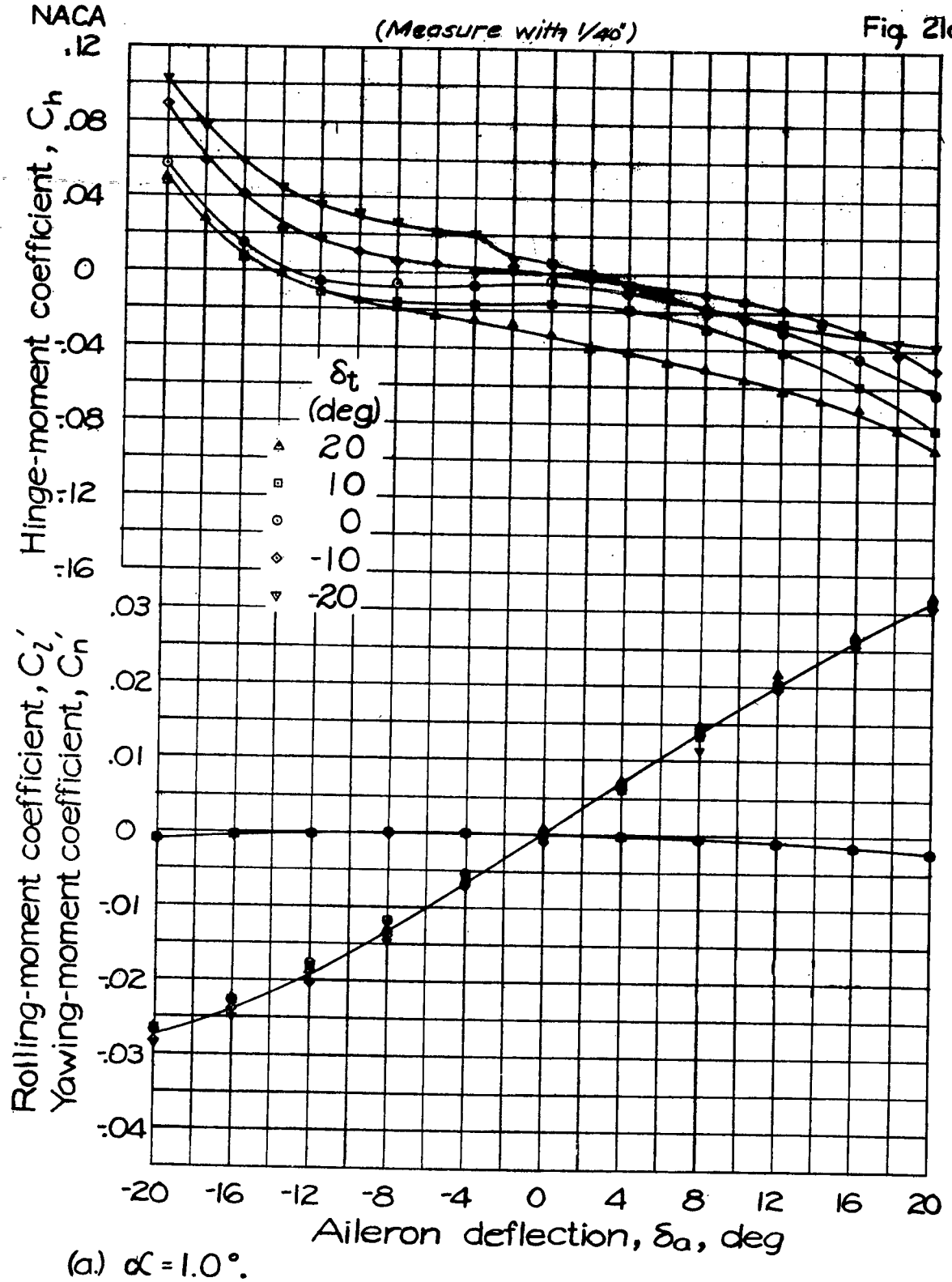


(a) $\alpha = 1.0°$.

FIGURE 21.- Effect of tab deflection on the aileron characteristics of the 0.40-scale model of a low-drag wing; $0.30c_a$ bevel aileron profile; no seal; 0.002c gaps.

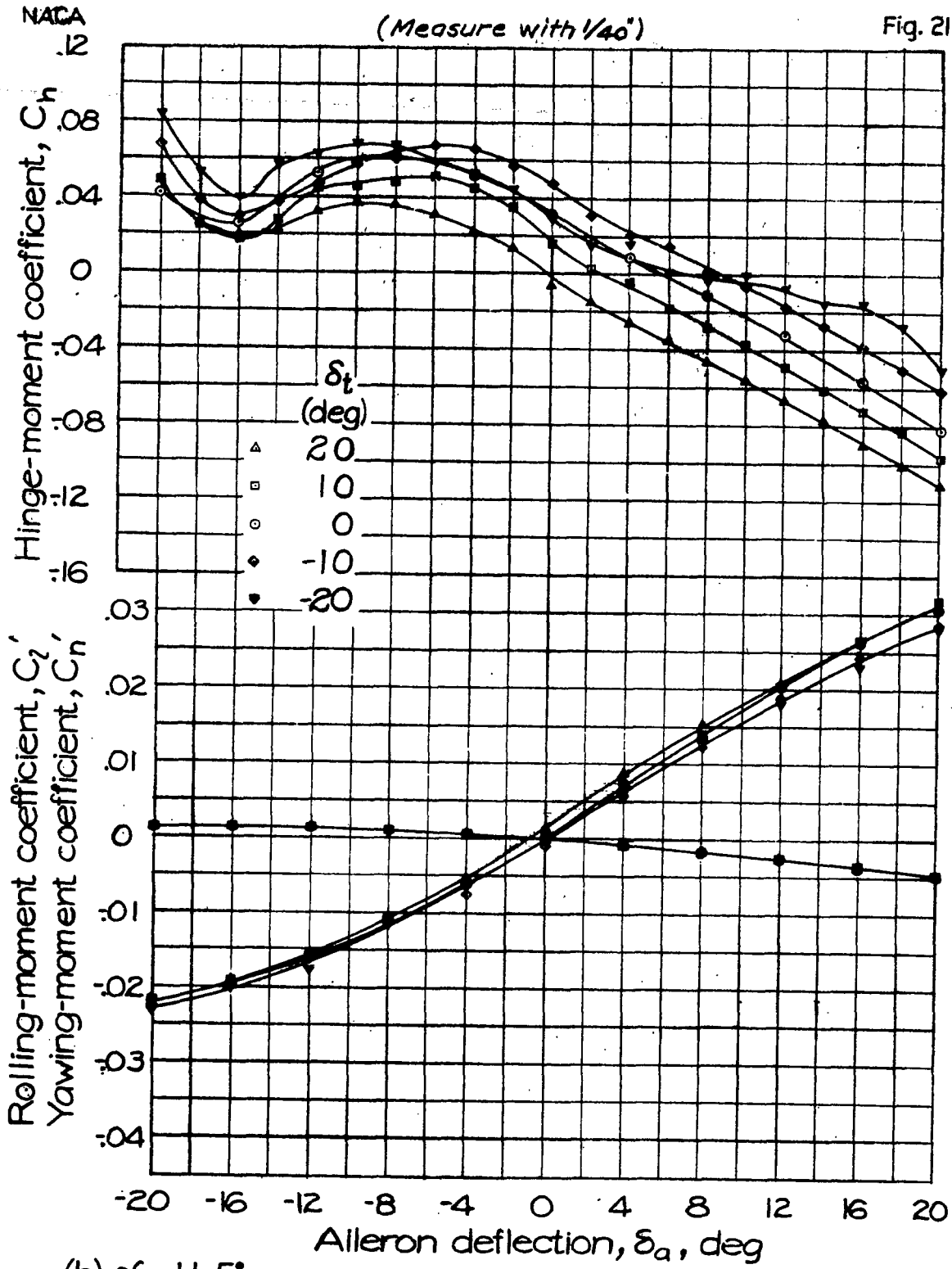


(b) $\alpha = 11.5°$.

FIGURE 21.- Concluded.

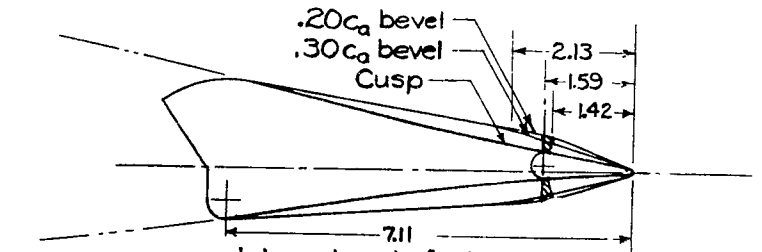


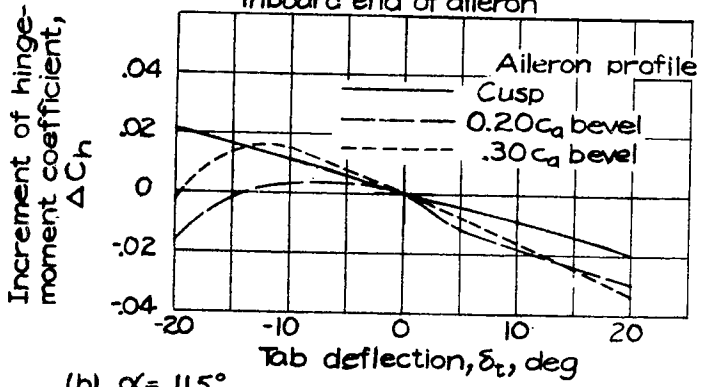


(b) $\alpha$ = 11.5°.

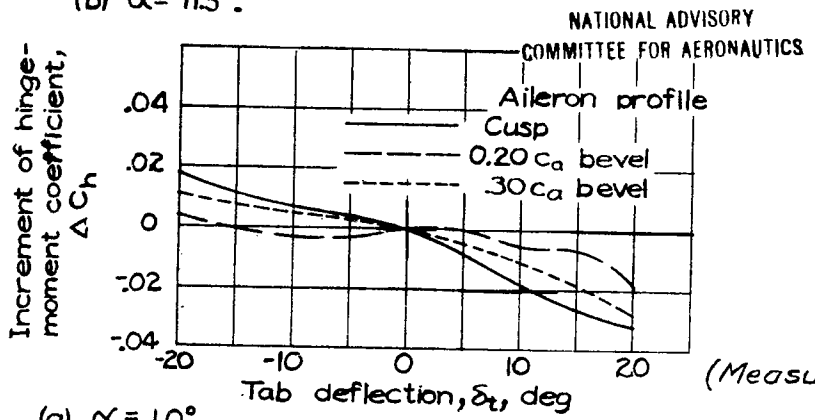


(a) $\alpha$ = 1.0°.

FIGURE 22.- Effect of aileron profile on the tab effectiveness; $\delta_a$=0°; cusp data from unpublished tests.

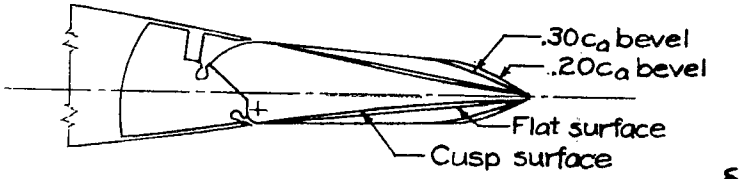


| Top surface | Bottom surface | Seal Gaps | $\delta_{a_{max}}$ (deg) |
|---|---|---|---|
| Cusp | Cusp | Top 0.004c | ±12.6 |
| Flat | Flat | Top .004c | ±13.2 |
| 0.30$c_a$ bevel | 0.30$c_a$ bevel | None .002c | ±14.9 |
| .20$c_a$ bevel | .20$c_a$ bevel | Bottom.004c | ±15.2 |
| .20$c_a$ bevel | .20$c_a$ bevel | Top .004c | ±15.2 |
| .20$c_a$ bevel | Cusp | Top .004c | ±12.5 |
| .20$c_a$ bevel | Cusp | Top .004c | 9.1, -15.4 |

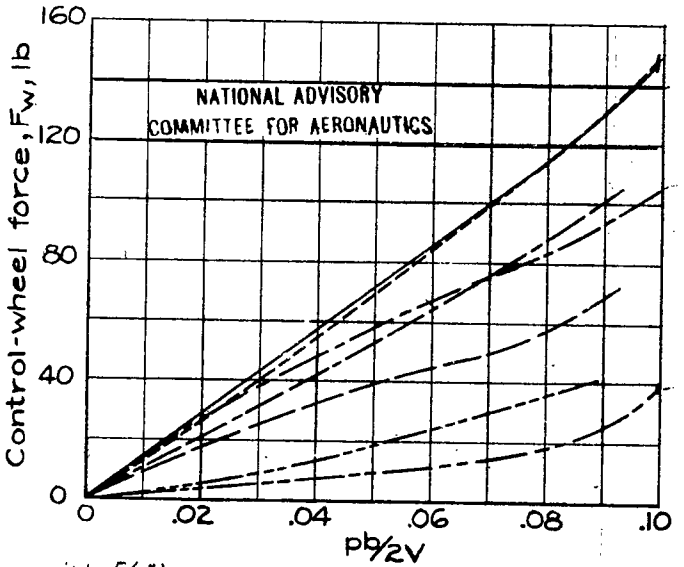


(Measure with 5/16")

FIGURE 26.- Effect of several modifications of the aileron profile on the control-wheel force of a high-speed airplane with a low-drag wing; $V_i$ = 306 mph.

Figs. 22, 26

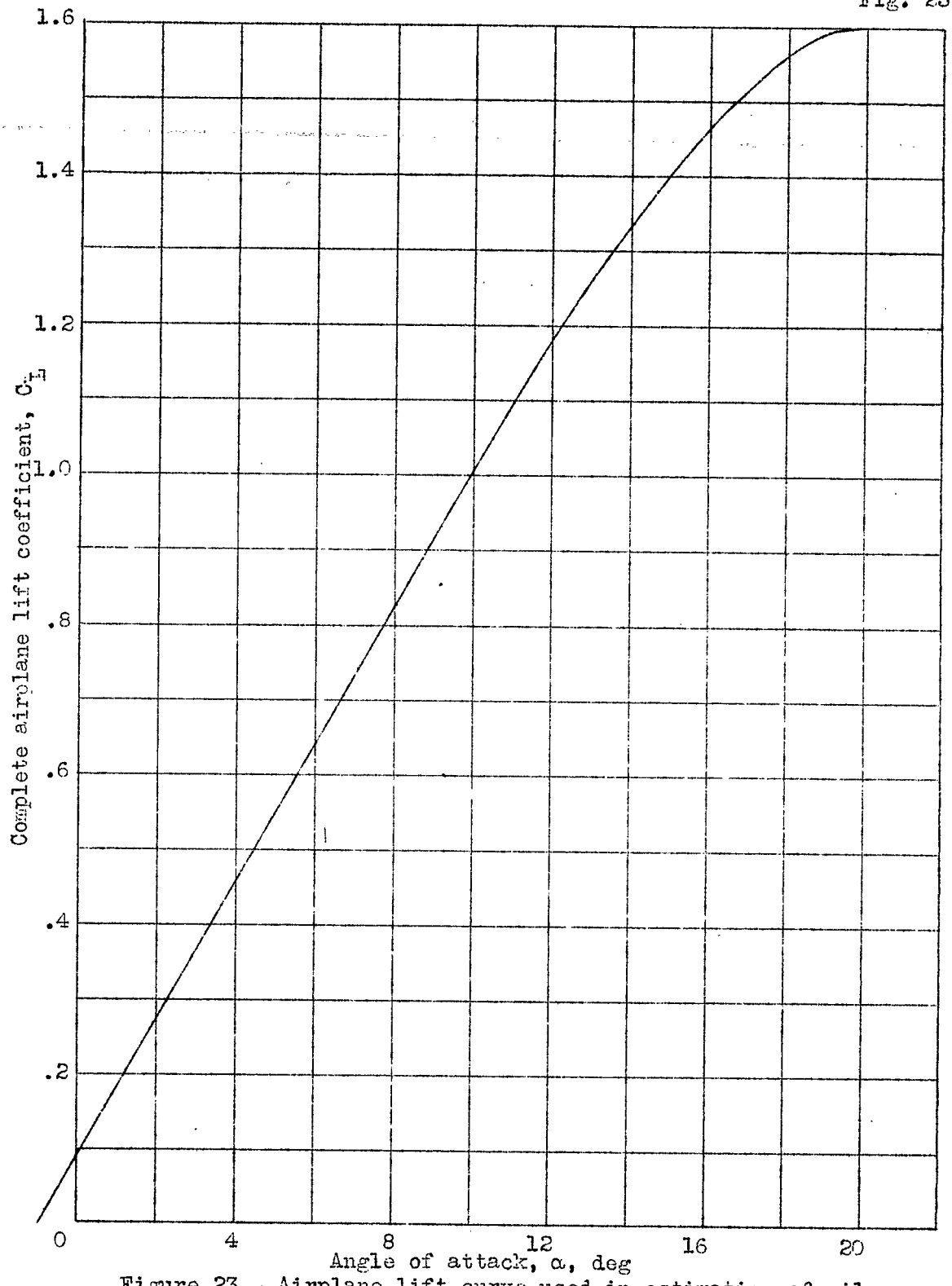


Figure 23.- Airplane lift curve used in estimation of aileron-control characteristics.

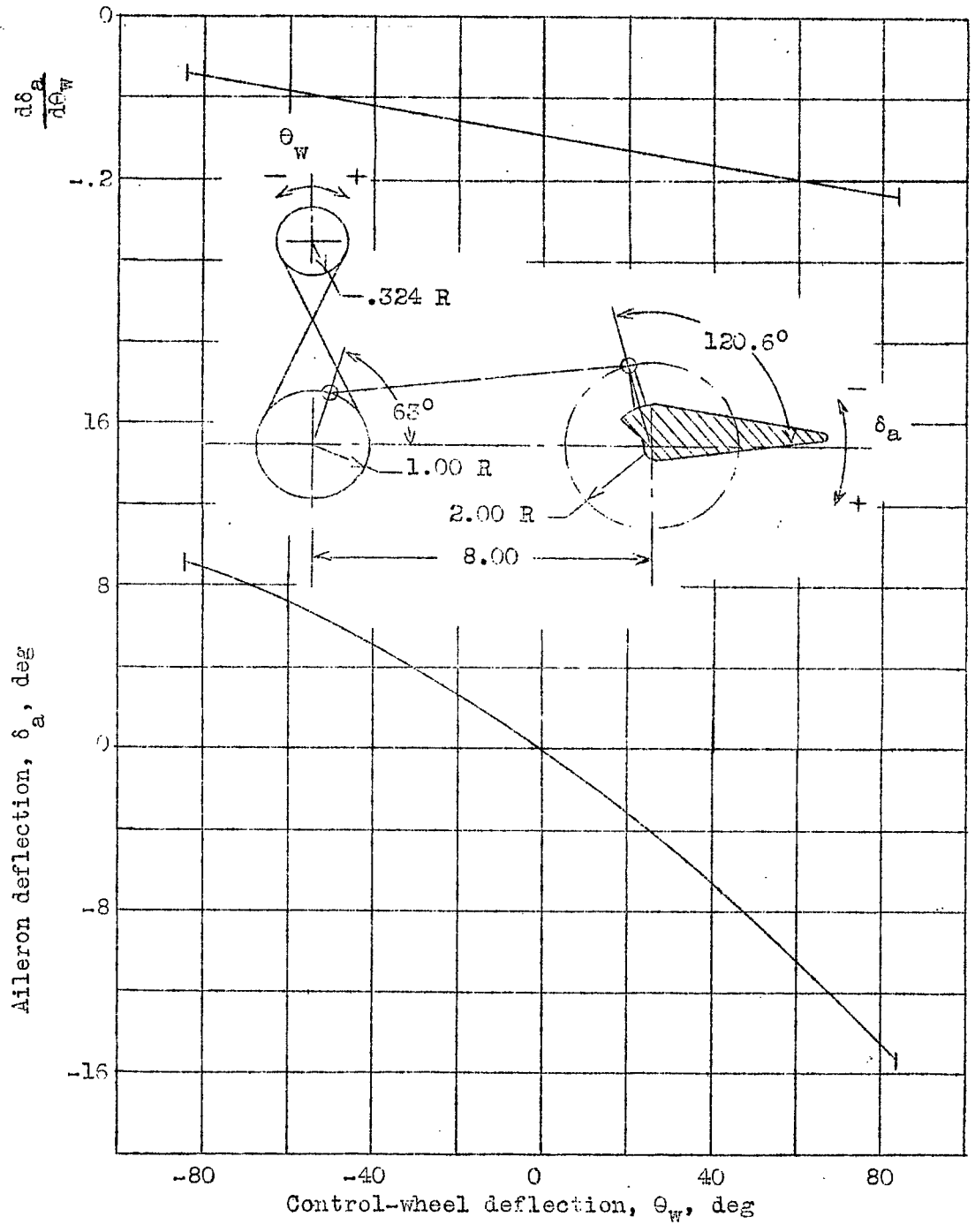


Figure 24.- Characteristics of assumed differential linkage.

Fig. 25a

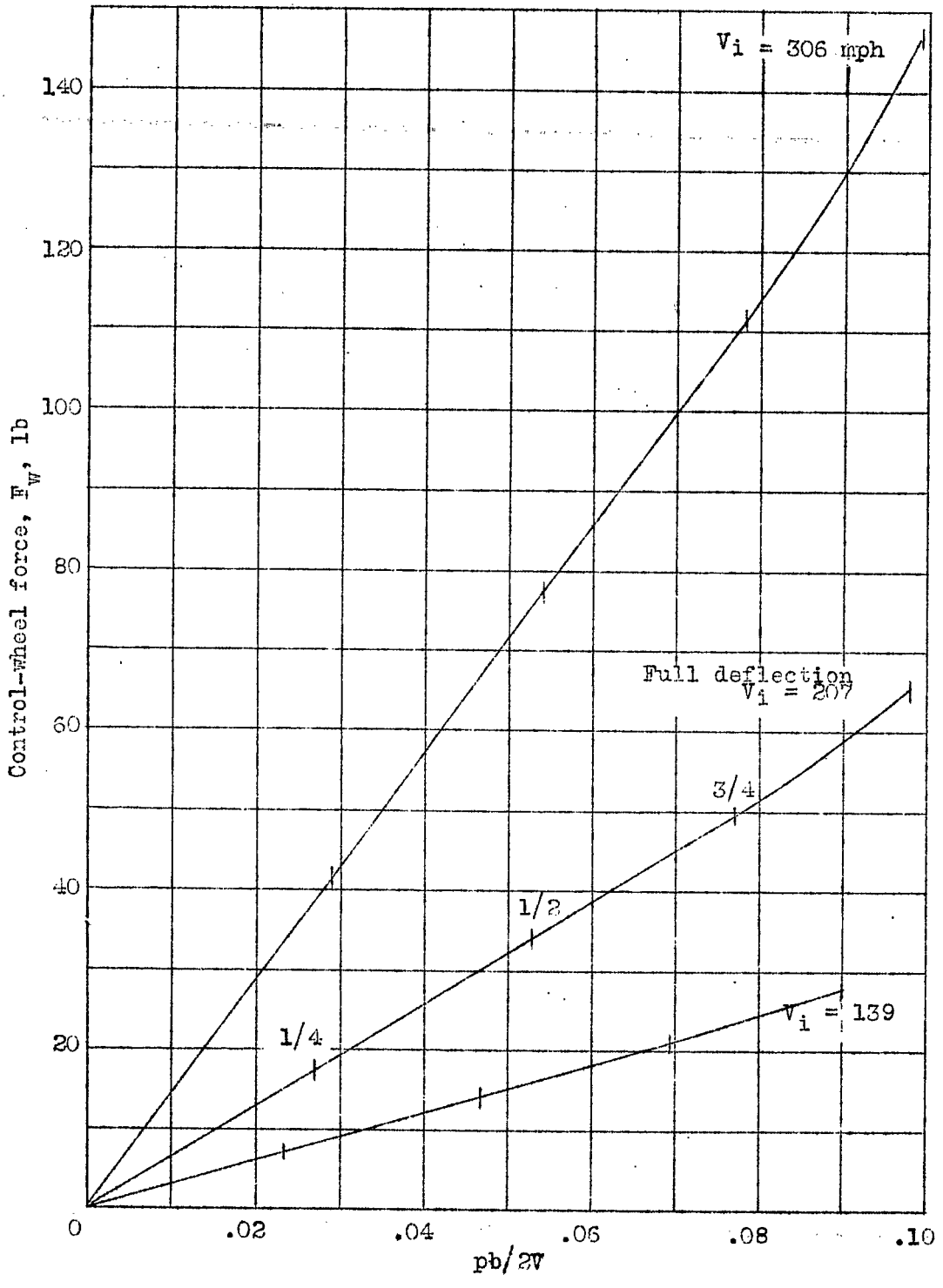


(a) Cusp ailerons; top seal; 0.004c gaps; $\delta_{a_{max}} = \pm 12.6°$.

Figure 25 a to e.- Aileron-control characteristics of a high-speed airplane with a tapered low-drag wing.

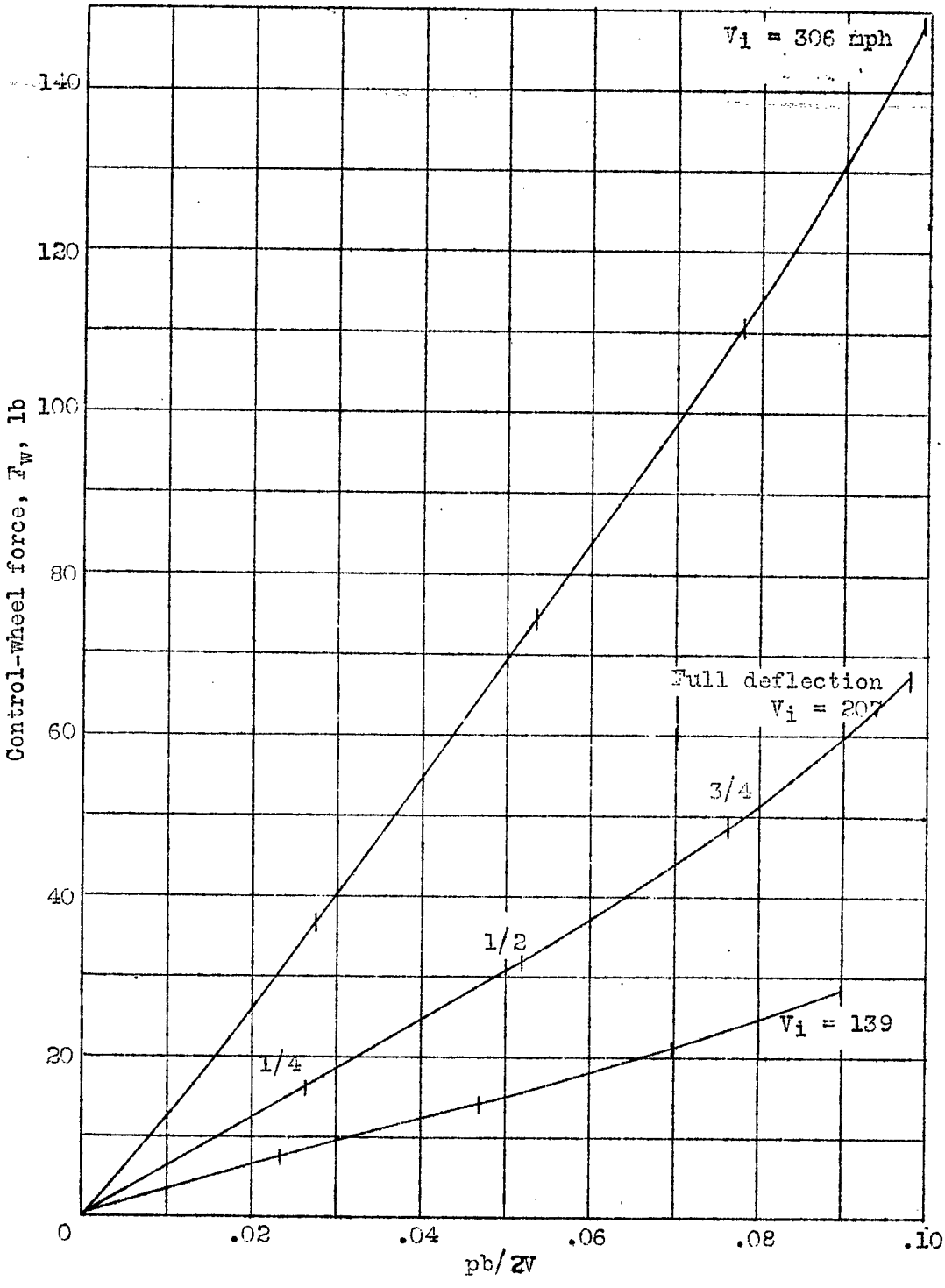


(b) Flat ailerons; top seal; 0.004c gaps; $\delta_{a_{max}} = \pm 13.2^\circ$.

Figure 25 .- Continued.

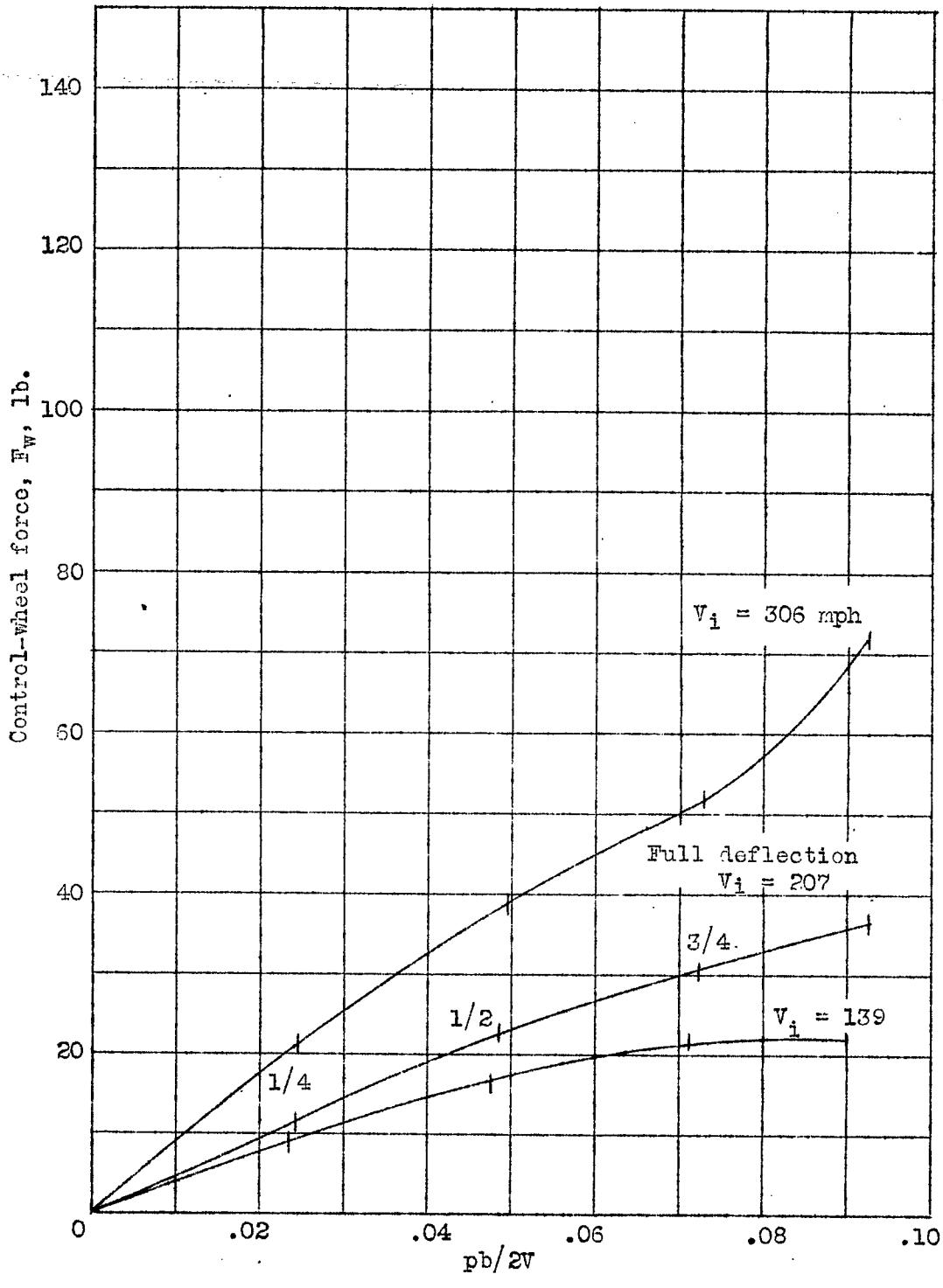


(c) $0.30c_a$ bevel ailerons; no seal; 0.002c gaps; $\delta_{a_{max}} = \pm 14.9°$.

Figure 25.- Continued.

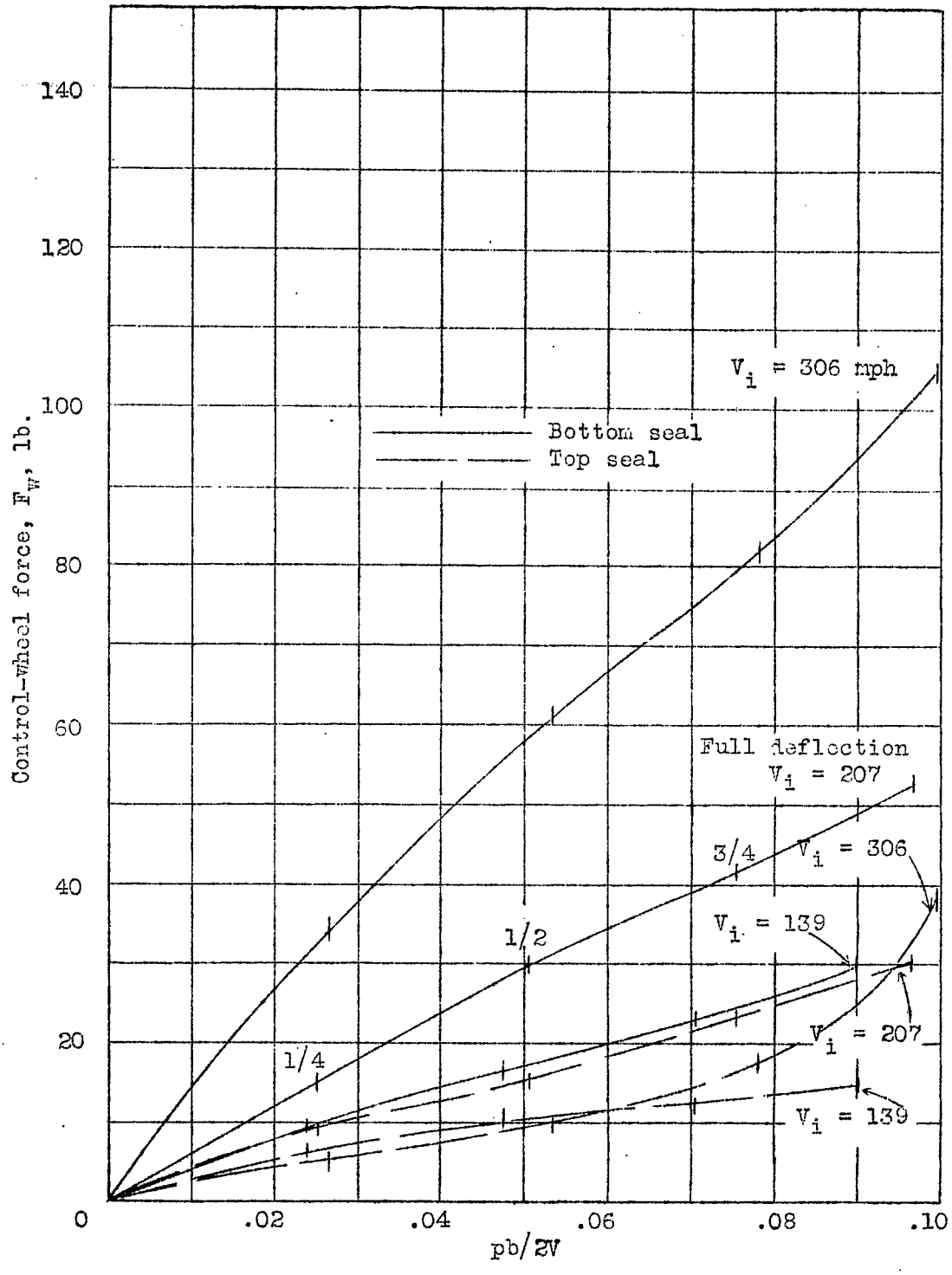


(d) $0.20c_a$ bevel ailerons; 0.004c gaps; $\delta_{a_{max}} = \pm 15.2°$.

Figure 25 .- Continued

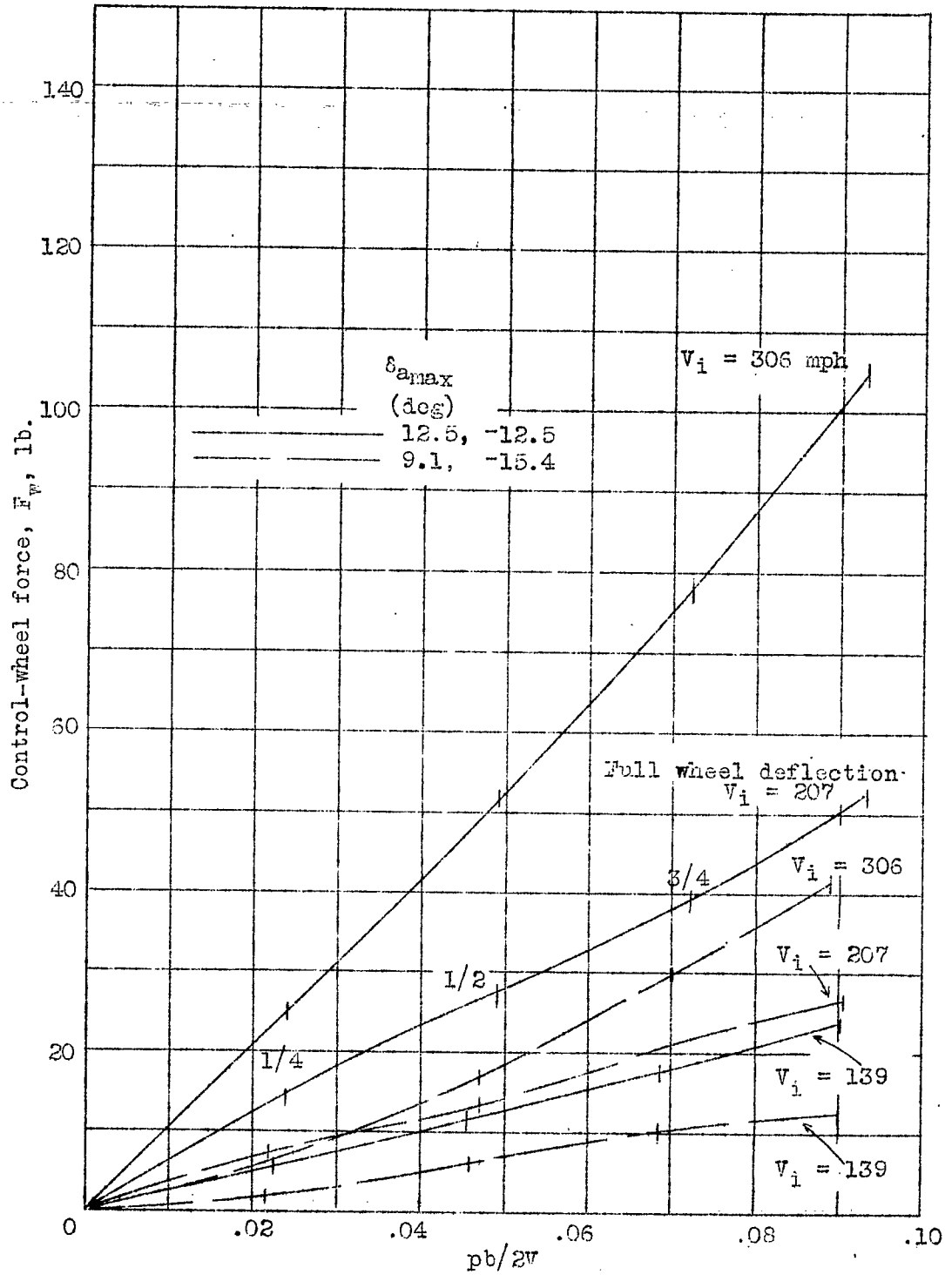


(e) $0.20c_a$ bevel top surface; cusp bottom surface; top seal; 0.004c gaps.

Figure 25 .- Concluded.

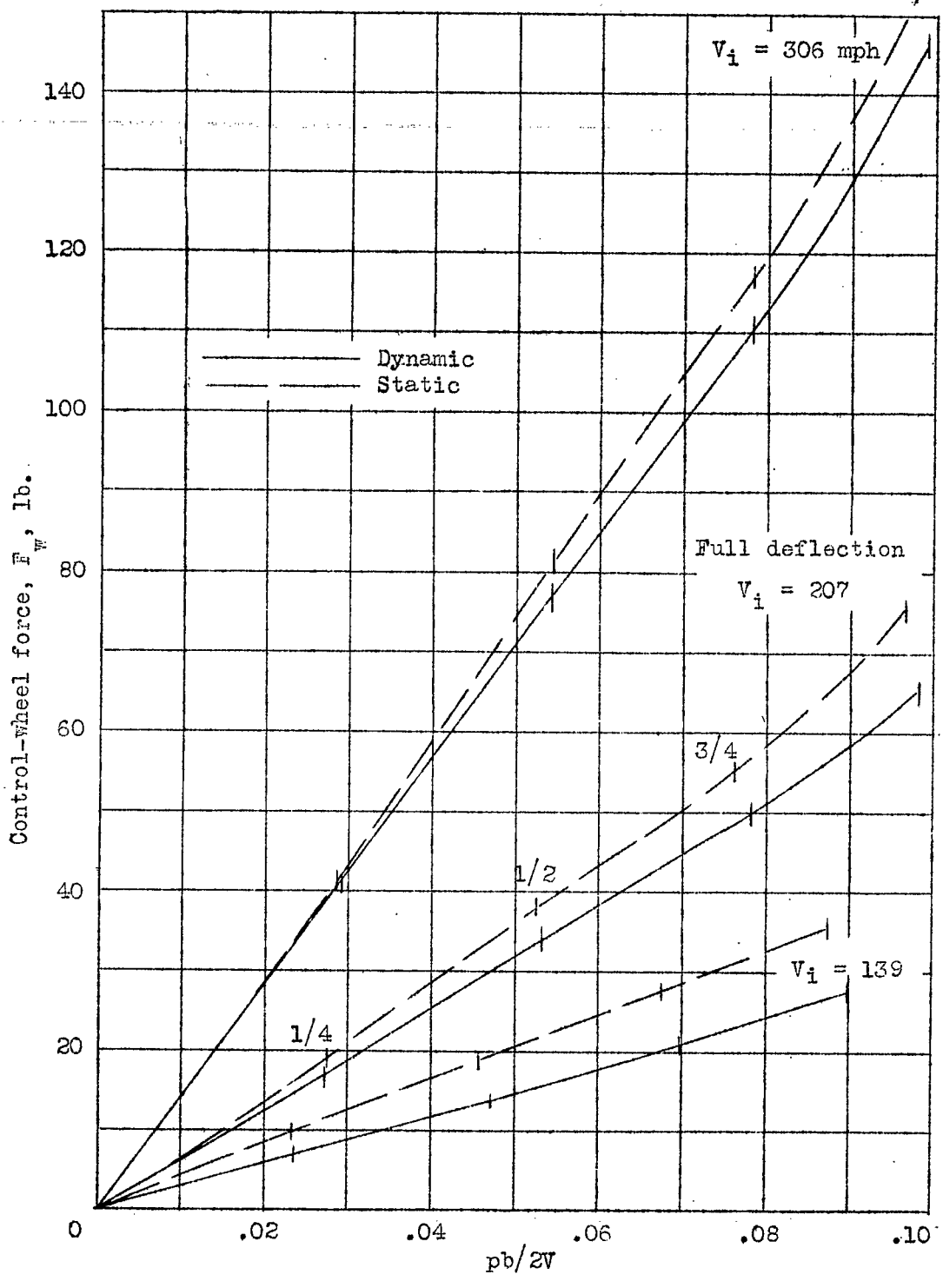


(a) Cusp ailerons; top seal; 0.004c gaps; $\delta_{a_{max}} = \pm 12.6^{\circ}$.

Figure 27a, b.- Effect of rolling on the wheel-force characteristics of a high-speed airplane with a tapered low-drag wing.

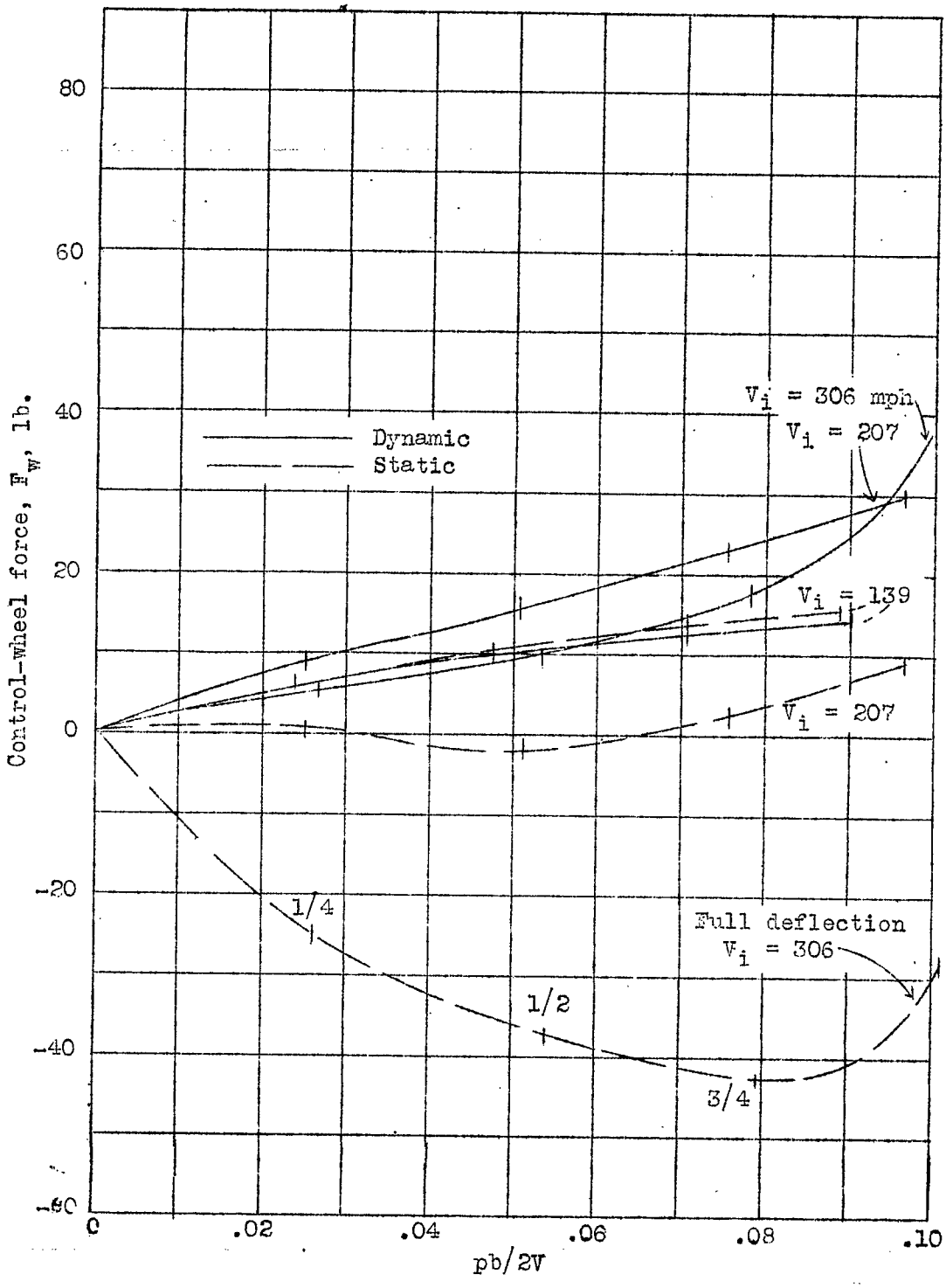


(b) $0.20c_a$ bevel ailerons; top seal; 0.004c gaps; $\delta_{a_{max.}} = \pm 15.2^\circ$.

Figure 27 .- Concluded.